





Article

Performance Optimization of a Ten Check MPPT Algorithm for an Off-Grid Solar Photovoltaic System

Muhammad Mateen Afzal Awan ¹, Muhammad Yaqoob Javed ², Aamer Bilal Asghar ^{2,*}
and Krzysztof Ejsmont ^{3,*}

¹ Department of Electrical Engineering, University of Management and Technology Lahore, Sialkot 51310, Pakistan; mateen.afzal@skt.umt.edu.pk

² Department of Electrical and Computer Engineering, COMSATS University Islamabad, Lahore 54000, Pakistan; yaqoob.javed@cuilahore.edu.pk

³ Faculty of Mechanical and Industrial Engineering, Warsaw University of Technology, 02-524 Warsaw, Poland

* Correspondence: aamerbilal@cuilahore.edu.pk (A.B.A.); krzysztof.ejsmont@pw.edu.pl (K.E.)

Abstract: In order to operate a solar photovoltaic (PV) system at its maximum power point (MPP) under numerous weather conditions, it is necessary to achieve uninterrupted optimal power production and to minimize energy losses, energy generation cost, and payback time. Under partial shading conditions (PSC), the formation of multiple peaks in the power voltage characteristic curve of a PV cell puzzles conventional MPP tracking (MPPT) algorithms trying to identify the global MPP (GMPP). Meanwhile, soft-computing MPPT algorithms can identify the GMPP even under PSC. Drawbacks such as structural complexity, computational complexity, huge memory requirements, and difficult implementation all affect the viability of soft-computing algorithms. However, those drawbacks have been successfully overcome with a novel ten check algorithm (TCA). To improve the performance of the TCA in terms of MPPT speed and efficiency, a novel concept of data arrangement is introduced in this paper. The proposed structure is referred to as Optimized TCA (OTCA). A comparison of the proposed OTCA and classic TCA algorithms was conducted for standard benchmarks. The results proved the superiority of the OTCA algorithm compared to both TCA and flower pollination (FPA) algorithms. The major advantage of OTCA in MPPT stems from its speed as compared to TCA and FPA, with almost 86% and 90% improvement, respectively.

Keywords: maximum power point; partial shading condition; solar photovoltaic; MPPT algorithm



Citation: Awan, M.M.A.; Javed, M.Y.; Asghar, A.B.; Ejsmont, K.

Performance Optimization of a Ten Check MPPT Algorithm for an Off-Grid Solar Photovoltaic System.

Energies **2022**, *15*, 2104. <https://doi.org/10.3390/en15062104>

Academic Editor: Alessandro Cannavale

Received: 8 February 2022

Accepted: 10 March 2022

Published: 13 March 2022

Publisher's Note: MDPI stays neutral with regard to jurisdictional claims in published maps and institutional affiliations.



Copyright: © 2022 by the authors. Licensee MDPI, Basel, Switzerland. This article is an open access article distributed under the terms and conditions of the Creative Commons Attribution (CC BY) license (<https://creativecommons.org/licenses/by/4.0/>).

1. Introduction

The diminution of fossil fuels, escalation of energy demand and greenhouse gas emissions, and mounting energy prices have pushed the world toward renewable energy sources. Solar energy is one of the key renewable energy sources that provide electricity without giving rise to any carbon dioxide emission [1]. Furthermore, a single-step conversion of sunlight into electricity using a solar photovoltaic (PV) cell (made up of semiconductor materials, mostly silicon [2]) using the photoelectric effect makes it the most easily accessible, cheap, and reliable renewable energy solution [3]. To generate maximum possible power, it is necessary to continuously operate the PV cell at its MPP [4]. Therefore, an MPP tracker governed by an algorithm is employed [5]. Common conventional algorithms include: perturb and observe [6], incremental conductance [7], fractional open circuit [8], and fractional short circuit [9]. Such algorithms are simple to understand and cheap to implement; however, there are significant drawbacks including system dependence, steady-state oscillations, and inability to perform under partial shading conditions (PSC). Multiple improvements have been made over the years to enhance the performance of conventional algorithms under different weather conditions. One of such improvements was the variable step size P&O algorithm, which was introduced in [10–14]. It starts with a big step size to reach the MPP in minimum time, and then gradually reduces the step size to

achieve the MPP with higher efficiency, as this reduces the tracking time. Another approach entailed modeling hardware with a DSP controller to enable the conventional HC technique to perform under PSC [15], which facilitated a 17.5% improvement in the convergence speed. Another idea of variable step size InC algorithm was adopted in [16]. The almost same strategy is implemented in [17] using PIC16F877A controller. An improved FSCC algorithm was proposed in [18] where short circuit current was measured using preset current thresholds. A switched semi-pilot cell was used to measure open-circuit voltage of a PV array and to improve the efficiency of the FOCV algorithm [19].

Conversely, the best known soft-computing algorithms include: fuzzy logic [20], genetic [21], cuckoo search [22], ant colony [23], artificial neural network [24,25], differential evolution [26], particle swarm optimization [27], grey wolf optimization [28], artificial bee colony [29], and flower pollination [4]. The main advantages of metaheuristic/soft-computing algorithms include zero steady-state oscillations and the ability to track MPP under PSC, while their primary disadvantages are mainly due to high implementation costs, huge memory requirements, structural complexity, need for extensive data training, etc. Numerous improvements have already been introduced to soft-computing algorithms, for instance the “new rule compressed fuzzy logic method” presented in [30], which improved MPPT efficiency and tracking speed. The methodology proposed in [30] was evaluated using an experimental setup. ANN is typically integrated with metaheuristic and conventional algorithms due to its extensive optimization scope [31,32]. A modified PSO algorithm achieved reduced steady-state oscillations, more accurate results, and faster response in [33]. A noticeable improvement in tracking speed and efficiency was achieved by integrating FPA with a chaos-map in [34].

A brief overview of the best known and most used conventional and soft-computing MPPT algorithms is presented in Figure 1. Under PSC, the formation of multiple peaks in the power–voltage (P–V) characteristic curve of a PV cell prevents conventional MPPT algorithms from identifying the GMPP [35]. Meanwhile, soft-computing MPPT algorithms are able to handle this problem and converge close to the GMPP [36]. However, soft-computing algorithms are typically not without major problems themselves, mainly in terms of their (1) structural complexity, (2) computational complexity, (3) implementation complications, and (4) huge memory prerequisites [4].

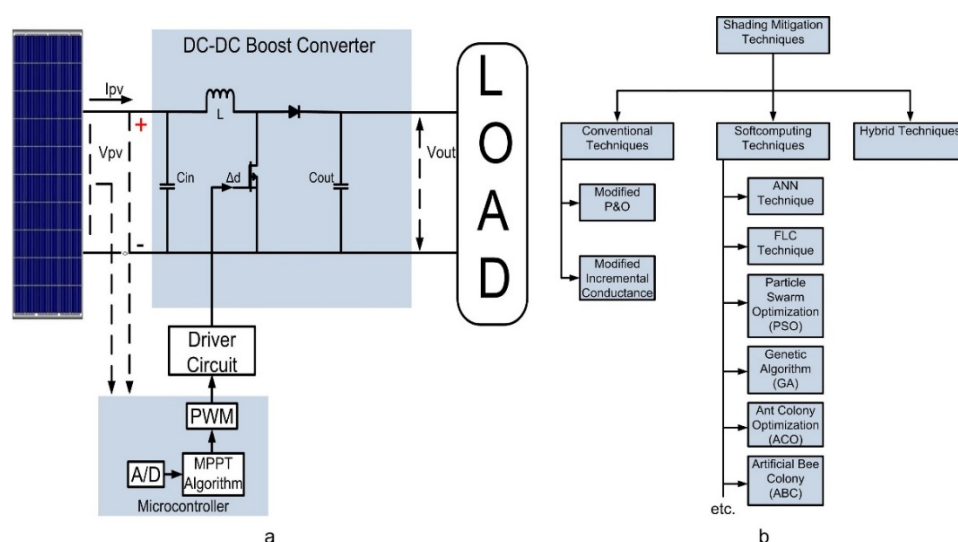


Figure 1. Solar photovoltaic system with MPPT algorithms (a) Basic block diagram of PV system. (b) Various MPPT algorithms in solar PV systems.

However, this can change with the introduction of the novel “ten check algorithm (TCA)” proposed in [37], which successfully overcame the above-mentioned drawbacks of soft-computing MPPT algorithms. After performing the SWOT (strength, weakness, opportunity, threats) analysis for the TCA, we realized that the random generation and

application of solutions to the MPP tracker increases the settling time and reduces the MPP tracking speed of TCA. To overcome these weaknesses, we proposed the inclusion of “data arrangement” in the structure of TCA to improve its MPP tracking speed, MPPT efficiency, and settling time of output power.

The well-established metaheuristic FPA and TCA, as well as the proposed OTCA algorithms, were evaluated at a standalone solar PV system under diverse weather conditions. The results evidenced superiority of the proposed OTCA algorithm over the TCA in terms of MPP tracking speed, MPPT efficiency, and settling time of output power.

The paper is organized as follows: Section 2 describes the TCA algorithm, details the SWOT analysis conducted for the TCA, and posits the problem statement. Section 3 introduces the optimized Ten Check algorithm. Section 4 discusses the results obtained for the TCA and OTCA algorithms. Section 5 outlines our conclusions and directions for further study.

2. Ten Check Algorithm

The TCA algorithm operates in the following order: (1) generation, (2) scaling, and (3) application of uniformly distributed random solutions. It initiates random solutions (range 0–1) and scales them in the predefined limits of the controlling variables (A and B). Subsequently, the scaled solutions are sent to the duty cycle input of the DC/DC converter. The solution with the highest power output is selected as the regional best (RB) of a relative iteration and is saved in a set of local solutions. The number of iterations is dependent on the controlling variables. In the final iteration, the RB with the highest power yield within the set is selected as the universal best (UB).

Changes in the voltage (ΔV) or current (ΔI) indicate changes in weather conditions. The thresholds for ΔV and ΔI are set at 0.2 V and 0.1 A, respectively, using the hit and trial method [37]. The mathematical equations for ΔV and ΔI are presented in Equations (1) and (2), respectively. The flowchart of the TCA algorithm is presented in Figure 2.

$$\Delta V = \frac{V_{pv}(t) - V_{pv}(t-1)}{V_{pv}(t)} \geq 0.2 \quad (1)$$

$$\Delta I = \frac{I_{pv}(t) - I_{pv}(t-1)}{I_{pv}(t)} \geq 0.1 \quad (2)$$

2.1. SWOT Analysis for the TCA Algorithm

The purpose of the SWOT analysis is to judge the technical viability of the TCA MPPT algorithms. The SWOT analysis is presented in Table 1.

2.2. Problem Statement

The ability to track the MPP using multiple concepts of randomization is the advantage offered by soft-computing MPPT algorithms under PSC. However, randomization also has downsides related to long settling times and complex implementation. To overcome these weaknesses without affecting the strength of randomization, we proposed the concept of “data arrangement”. Randomly generated data are arranged in a specific order such that the step size between two consecutive solutions becomes minimized to reduce the settling time of output power, reduce the MPP tracking time, and simplify the implementation similarly to conventional algorithms. Additionally, the method can increase the MPP tracking speed and efficiency.

Table 1. SWOT analysis of TCA algorithm.

| Strengths | Weaknesses | Opportunities | Threats |
|--|--------------------|--|---------|
| Simple structure | Hard to implement. | Improvement in tracking speed | Nil |
| No huge computations | High settling time | Improvement in tracking accuracy | |
| Easy implementation | | Minimize the settling time to reduce the tracking time | |
| Fast tracking speed | | | |
| No parameter to tune | | | |
| Ability to differentiate MPP and GMPP | | | |
| Efficient performance under all weather conditions | | | |
| Independent of PV system | | | |
| Zero steady-state oscillations | | | |

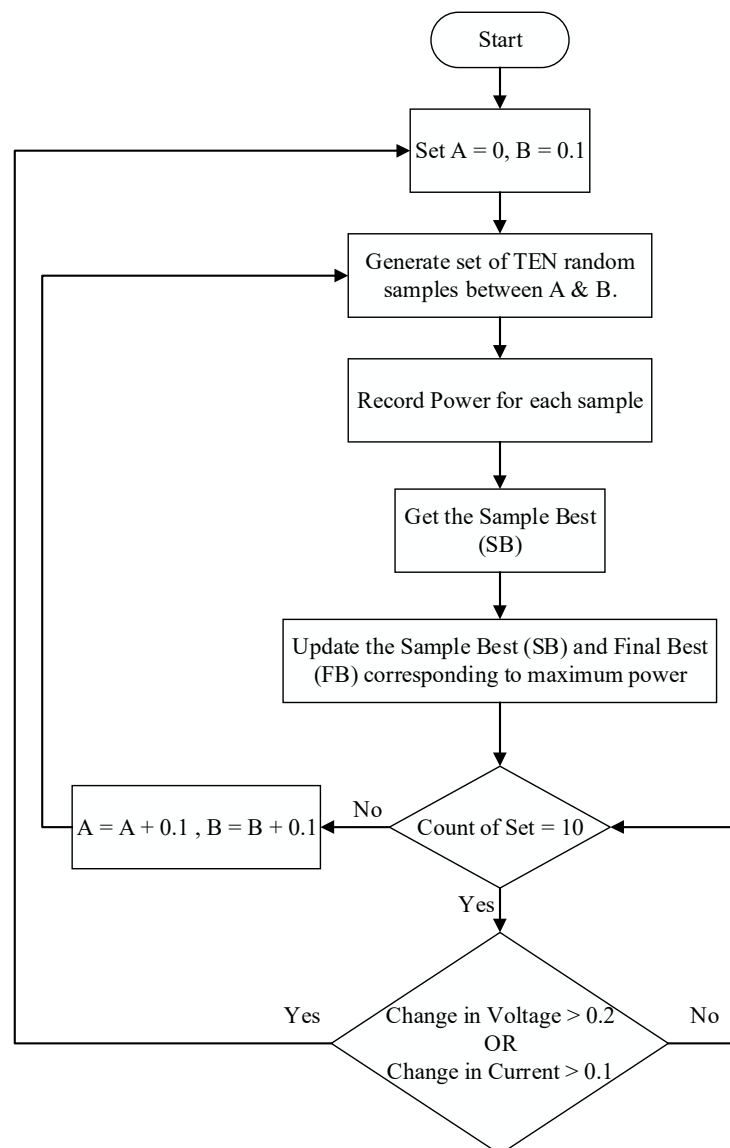


Figure 2. Flowchart of the ten check algorithm.

3. Optimized TCA

The novel strategy of the proposed OTCA algorithm entails “data arrangement” of randomly generated solutions to reduce the settling time of output power and to reduce the MPP tracking time of the algorithm. It is structurally simple and easily implemented, requires no complex computations or excessive memory space, and yields no power spikes on transitions.

The OTCA initiates random solutions (range 0–1) within the predefined limits of controlling variables (A and B) and arranges them in descending order before forwarding them to the duty cycle input of the DC/DC converter. The descending arrangement facilitates quick stabilization of output power by reducing the settling time, which consequently also reduces tracking time. The solution with the maximum power output is selected as the regional best (R_B) of the relative iteration. The number of iterations depends on the controlling variables. In the final iteration, the R_B with the highest power in the set is selected as the universal best (U_B). The change in weather will be detected using Equations (1) and (2). The flowchart of the proposed OTCA algorithm is presented in Figure 3.

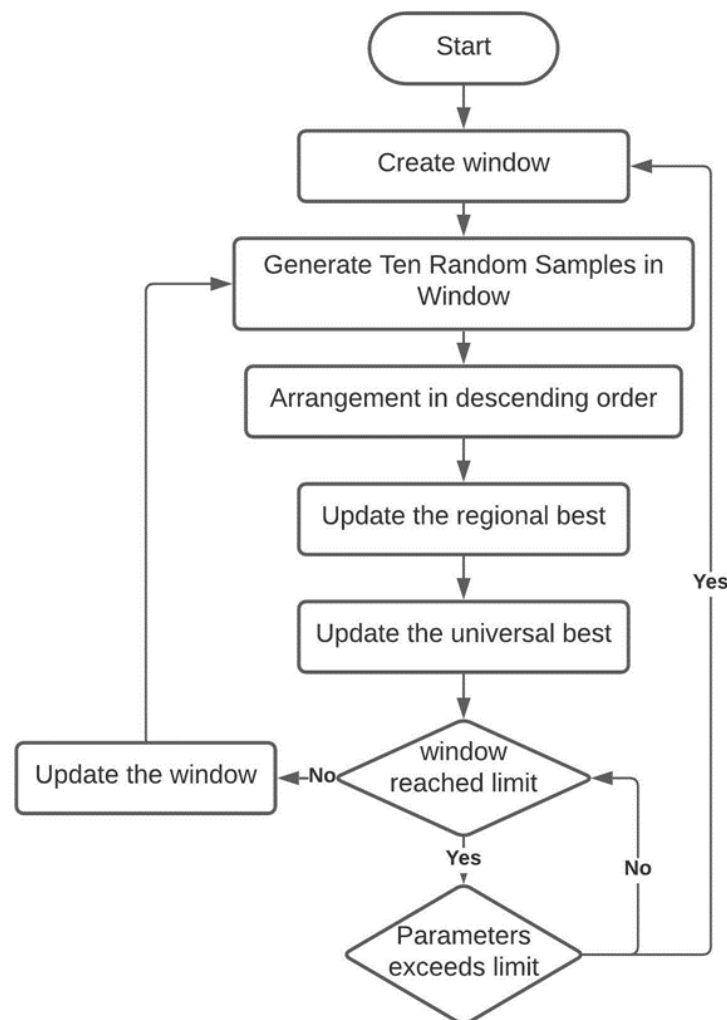
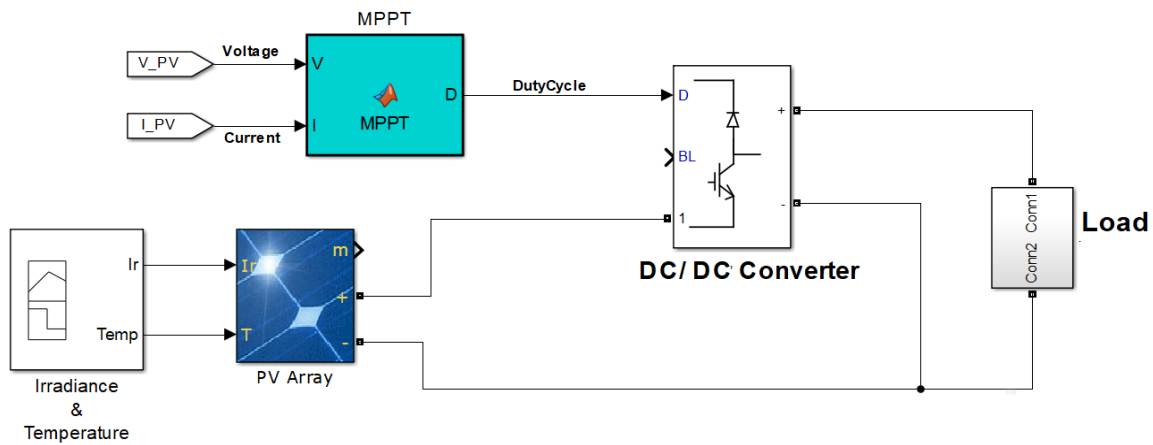


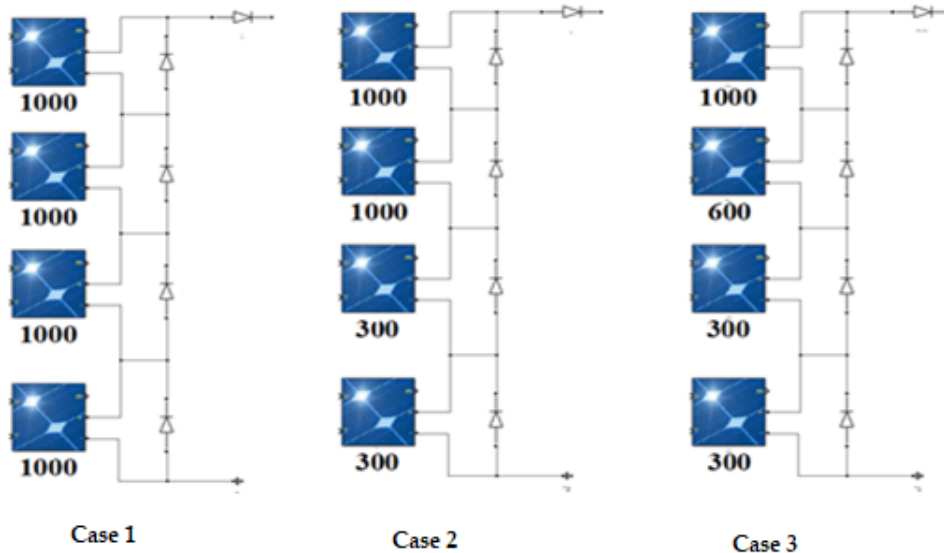
Figure 3. Flowchart of the optimized ten check algorithm.

4. Results and Discussion

The performance of the proposed OTCA was compared to that of the standard TCA at a 4S standalone solar PV system under varying weather conditions. The simulated model along with the 4S PV array is presented in Figure 4. The tuning parameters of both algorithms are presented in Table 2.



(a)



(b)

Figure 4. The 4S standalone solar photovoltaic testing system: (a) standalone photovoltaic system; (b) 4S PV array under zero, weak, and strong PSC.

Table 2. Tuning parameters of OTCA and TCA algorithms.

| Optimized Ten Check Algorithm | Ten Check Algorithm |
|-------------------------------|---------------------|
| A | A |
| B | B |

4.1. Uniform Weather Condition

Under uniform weather conditions, the existence of one peak in the characteristic curve streamlines the MPP tracking process for an algorithm. The MPP in Figure 5 occurred at 40 V, 3 A, and 120 W. The power extracted by the FPA, TCA, and the proposed OTCA algorithms was 119.2, 119.7, and 120 W, in 0.7516, 0.4972, and 0.0682 s, with an efficiency of 99.33%, 99.75%, and 100%, respectively. The results of the simulation presented in Figure 6 evidence the superiority of the proposed OTCA algorithm over the FPA and TCA algorithms in terms of MPPT efficiency and MPP tracking speed, with improvement by 90.93%, and 86.3%, respectively, under zero shading. Additionally, the absence of

spikes yielded smoother results, reduced the settling time, and improved the efficiency and tracking speed of the proposed OTCA algorithm. The results are summarized in Table 3.

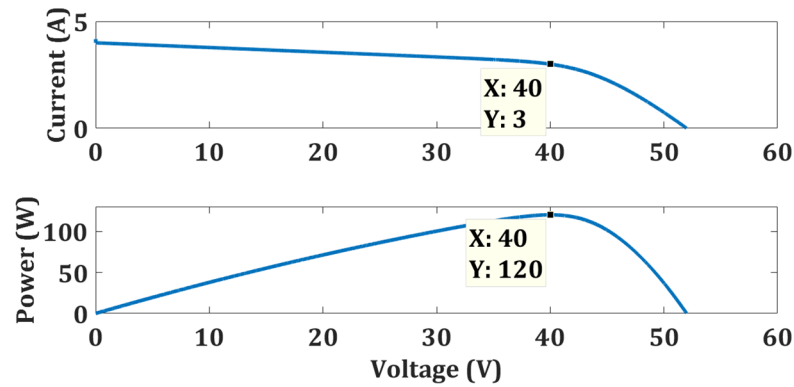
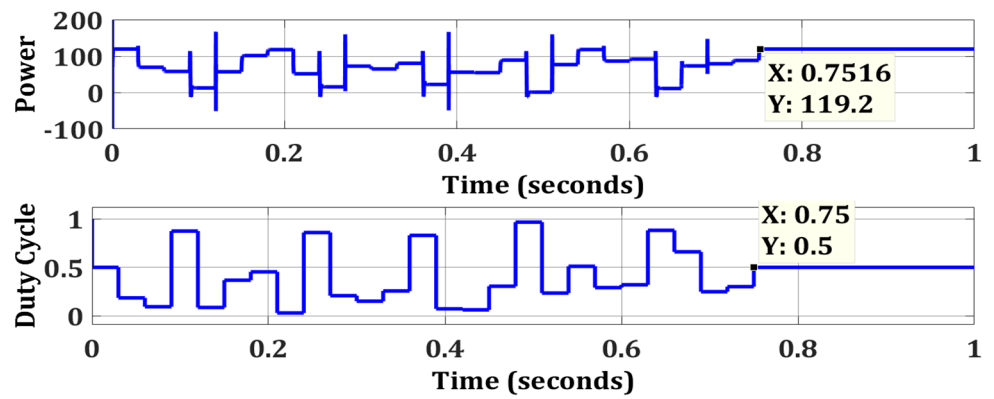
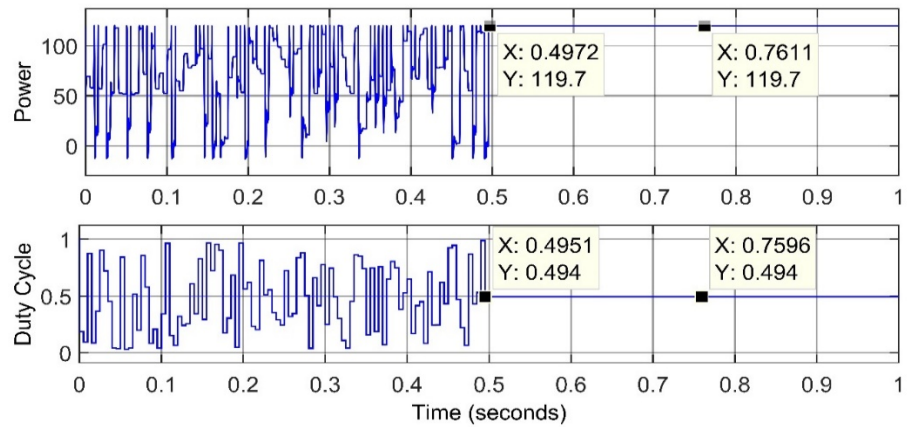


Figure 5. Characteristic curves of 4S PV array under zero shading.



(a)



(b)

Figure 6. Cont.

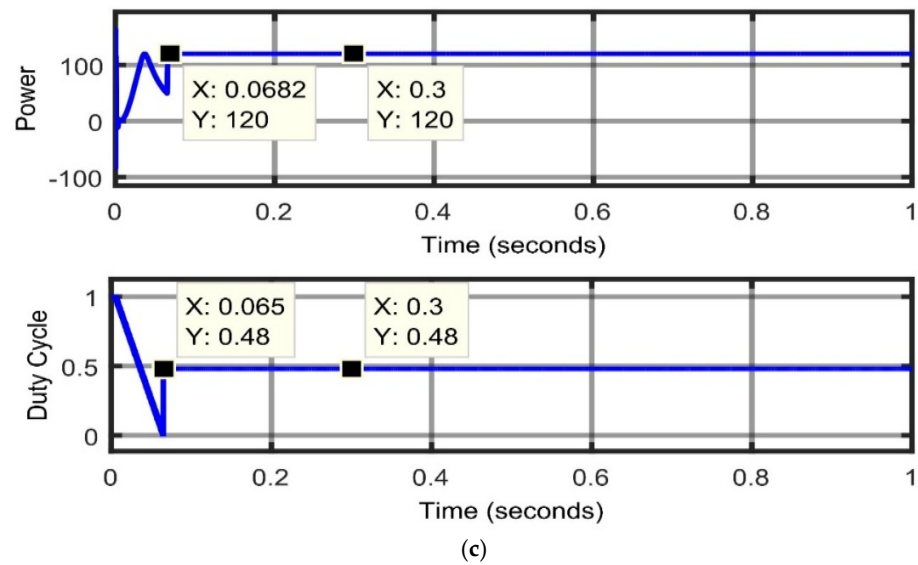


Figure 6. Results for FPA, TCA, and OTCA under zero shading. (a) FPA; (b) ten check algorithm; (c) optimized ten check algorithm.

Table 3. Performance comparison of FPA, TCA and OTCA under zero shading.

| Shading Patterns | Algorithms | P_{MPP} (W) | Rated Power (W) | Efficiency (%) | Tracking Time (s) | Increase in Tracking Speed (%) |
|------------------|------------|---------------|-----------------|----------------|-------------------|--------------------------------|
| Zero Shading | TCA | 119.7 | 120 | 99.75 | 0.4972 | 86.3 |
| | FPA | 119.2 | | 99.33 | 0.7516 | 90.93 |
| | OTCA | 120 | | 100 | 0.0682 | |

4.2. Weak Partial Shading

Under weak PSC, the formation of multiple peaks in the characteristic curves of a PV cell complicates MPPT processing for the operating algorithm. Complexity created due to the formation of multiple peaks in the characteristic curves of a PV array can be observed in Figure 7 under weak PSC. This non-linear behavior of the PV array confuses conventional algorithms when identifying the global MPP. The quantity of peaks depends on the number of shaded modules. The MPPs in Figure 8 occurred at 18.71 V, 2.983 A, and 55.81 W. The FPA, TCA, and the proposed OTCA algorithms attained a power of 55.24, 55.78, and 55.71 W in 0.7565, 0.497, and 0.071 s, with an efficiency of 98.98%, 99.95%, and 99.82%, respectively.

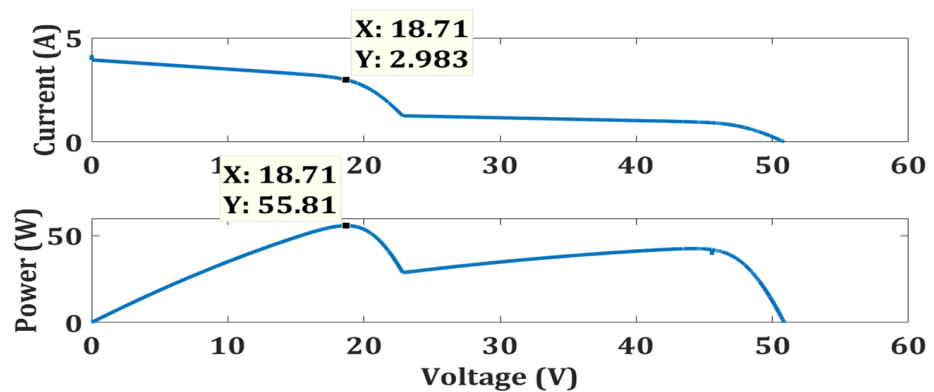


Figure 7. Characteristic curve of 4S PV array under weak partial shading.

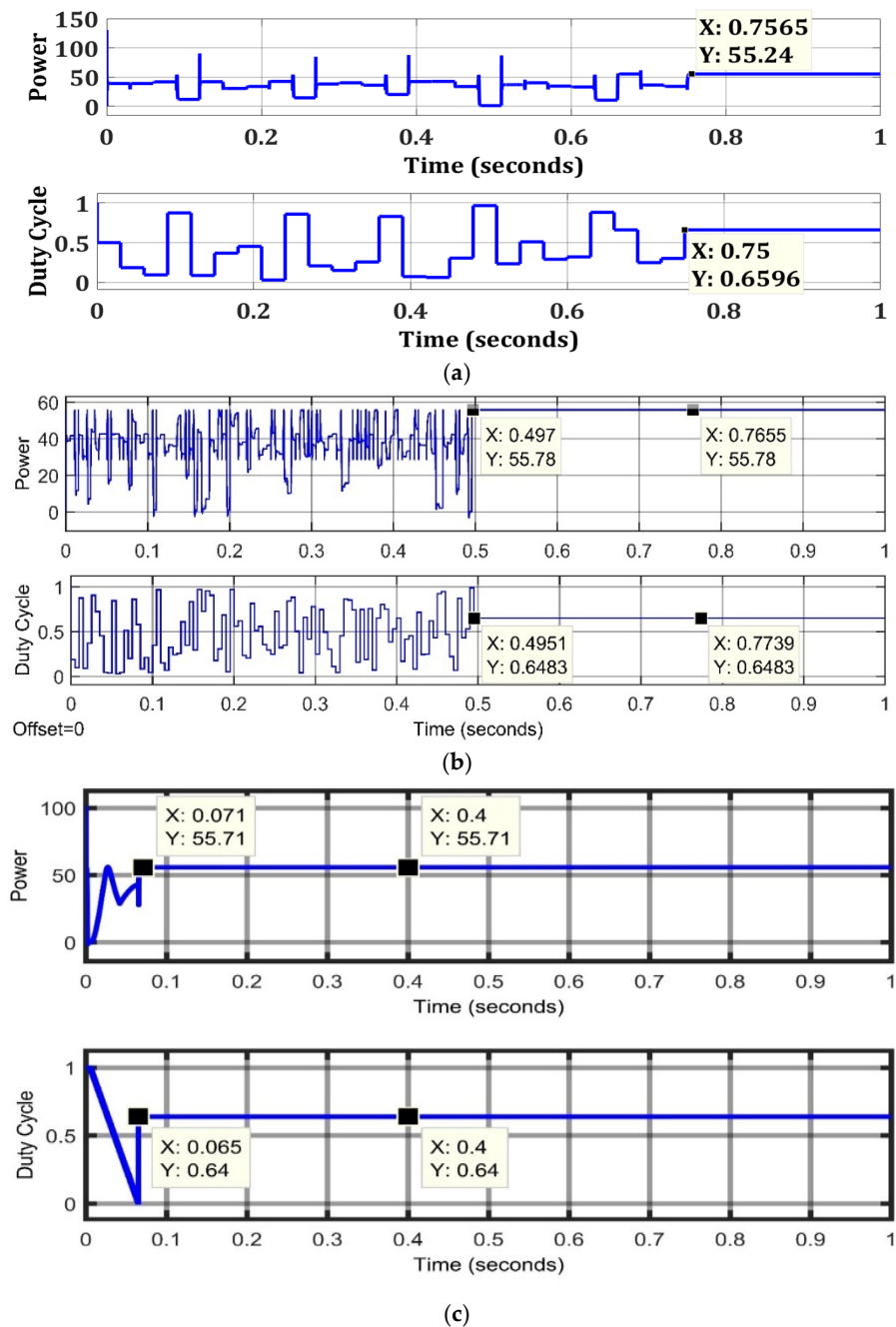


Figure 8. Results of FPA, TCA, and OTCA algorithms under weak partial shading: (a) FPA; (b) ten check algorithm; (c) optimized ten check algorithm.

A clear conceptual representation of FPA, TCA, and the proposed OTCA algorithm can be observed in Figure 8. Arrangement of the generated solutions in a descending order to avoid random application of solutions to the MPP tracker allowed OTCA to prove superior to the other two methods by reducing settling time and increasing MPP tracking speed. The simulation results presented in Figure 8 proved that the proposed OTCA algorithm outperformed the FPA and TCA algorithms in tracking speed by 90.61% and 85.7%, respectively, under weak PSC. Additionally, the absence of spikes smoothed the results, reduced the settling time, and improved the tracking speed of the proposed OTCA algorithm. The results are summarized in Table 4.

Table 4. Performance comparison of FPA, TCA, and OTCA algorithms under weak partial shading.

| Shading Patterns | Algorithms | P_{MPP} (W) | Rated Power (W) | Efficiency (%) | Tracking Time (s) | Increase in Tracking Speed (%) |
|----------------------|------------|---------------|-----------------|----------------|-------------------|--------------------------------|
| Weak Partial Shading | TCA | 55.78 | 55.81 | 99.955 | 0.497 | 85.7 |
| | FPA | 55.24 | | 98.98 | 0.7565 | 90.61 |
| | OTCA | 55.71 | | 99.82 | 0.071 | |

4.3. Strong Partial Shading

Under strong PSC, the MPPT becomes challenging due to the complexity of the characteristic curves model for the PV cell. Complications emerging due to the formation of multiple peaks in the characteristic curves of the PV array can be observed in Figure 9 under strong PSC. This non-linear behavior of the PV array confuses conventional algorithms when identifying the global MPP. The quantity of peaks depends on the number of shaded modules. The MPP in Figure 9 occurred at 43.91 V, 0.96 A, and 42.16 W. The FPA, TCA and the proposed OTCA algorithms attained 42.05, 42.16, and 42.15 W in 0.7527, 0.4972, and 0.066 s, with 99.74%, 100%, and 99.98% efficiency, respectively.

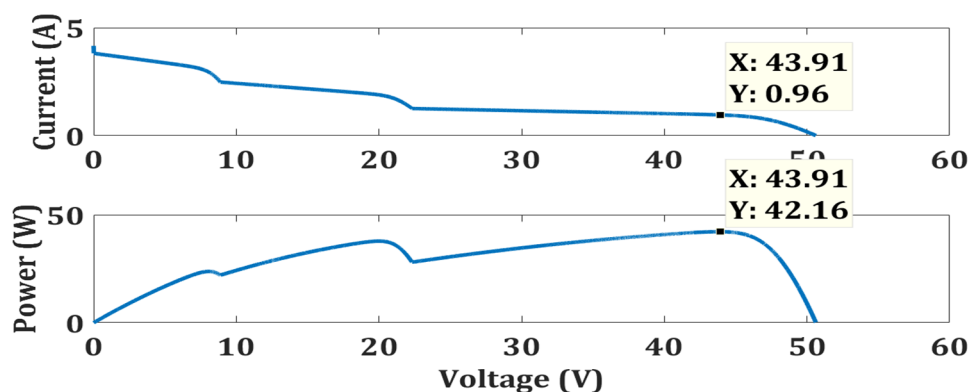


Figure 9. The characteristic curve of a 4S PV array under strong partial shading.

A clear conceptual representation of the FPA, TCA and the proposed OTCA is provided in Figure 10. Arrangement of the generated solutions in descending order to avoid random application in the MPP tracker allowed the OTCA to outperform the other two methods by reducing the settling time and increasing the MPP tracking speed. The simulation results presented in Figure 10 clearly indicate superiority of the proposed OTCA algorithm over FPA and TCA in terms of tracking speed by 91.23% and 86.7%, respectively, under strong PSC. Additionally, the absence of spikes yielded smoother results, reduced the settling time, and improved the tracking speed of the proposed algorithm. The results are summarized in Table 5.

Table 5. Performance comparison of FPA, TCA, and OTCA under strong partial shading.

| Shading Patterns | Algorithms | P_{MPP} (W) | Rated Power (W) | Efficiency (%) | Tracking Time (s) | Increase in Tracking Speed (%) |
|------------------------|------------|---------------|-----------------|----------------|-------------------|--------------------------------|
| Strong Partial Shading | TCA | 42.16 | 42.16 | 100 | 0.4972 | 86.7 |
| | FPA | 42.05 | | 99.74 | 0.7527 | 91.23 |
| | OTCA | 42.15 | | 99.98 | 0.066 | |

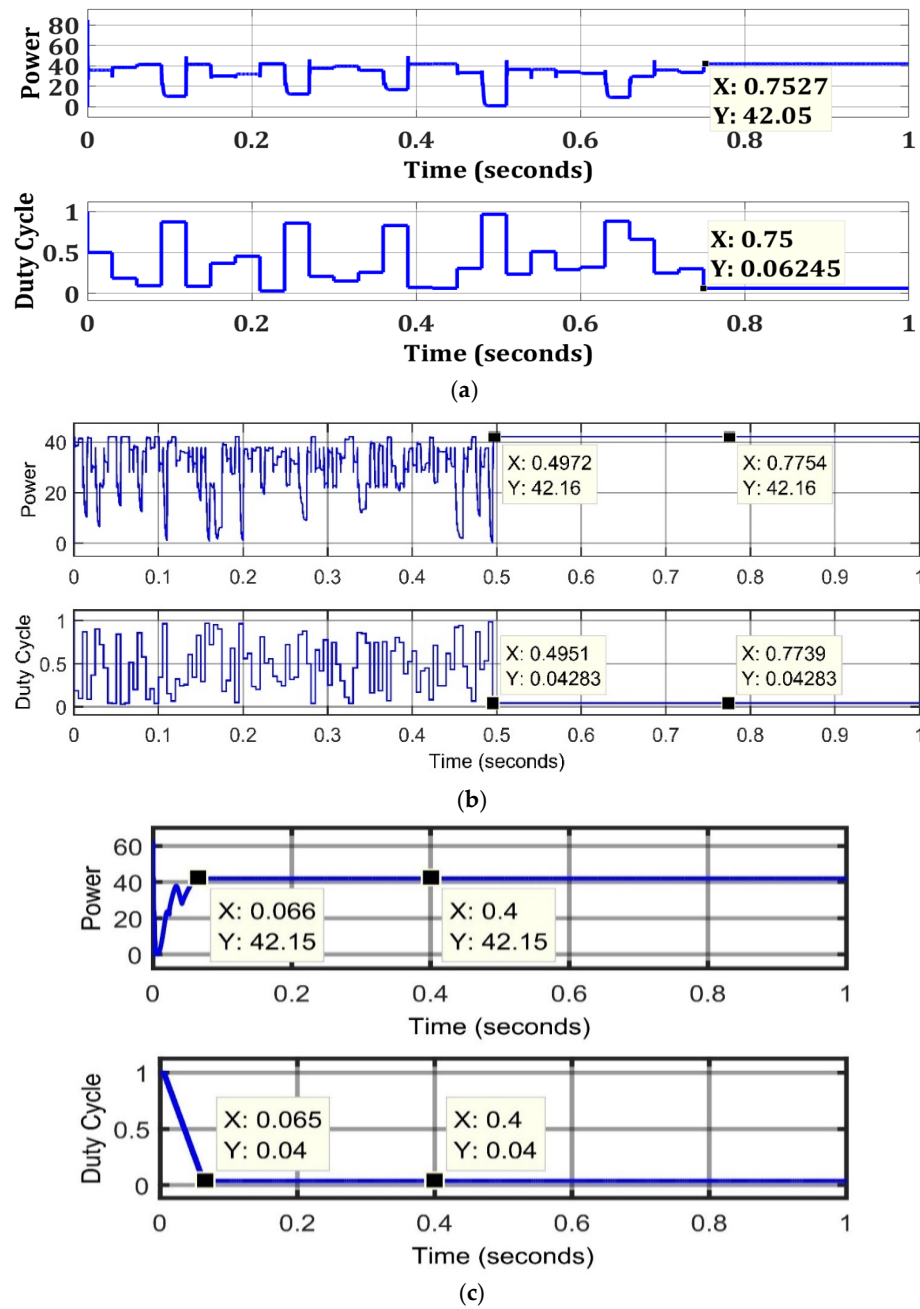


Figure 10. Results for FPA, TCA, and OTCA under strong partial shading: (a) FPA; (b) ten check algorithm; (c) optimized ten check algorithm.

4.4. Changing Weather Condition

The performance of the proposed OTCA algorithm was authenticated under continuously changing shading patterns (change occurred twice per second), and the results are presented and summarized in Figure 11 and Table 6, respectively. The proposed algorithm maintained its performance efficiency and MPPT speed under dynamically changing weather conditions, which demonstrated its suitability for MPPT in solar PV systems operating under changeable weather conditions.

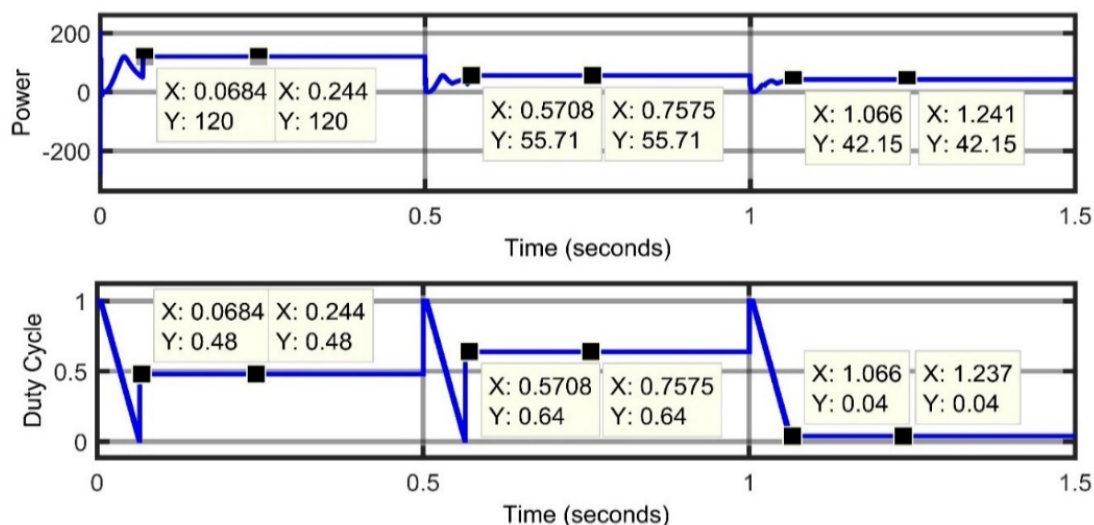


Figure 11. Authentication of OTCA under continuously changing weather conditions.

Table 6. Summary of results for the proposed OTCA MPPT algorithm.

| Shading Patterns | Algorithms | P_{MPP} (W) | Rated Power (W) | Efficiency (%) | Tracking Time (s) | Increase in Tracking Speed (%) |
|------------------------|------------|---------------|-----------------|----------------|-------------------|--------------------------------|
| Zero Shading | TCA | 119.7 | 120 | 99.75 | 0.4972 | 86.3 |
| | FPA | 119.2 | | 99.33 | 0.7516 | 90.93 |
| | OTCA | 120 | | 100 | 0.0682 | |
| Weak Partial Shading | TCA | 55.78 | 55.81 | 99.955 | 0.497 | 85.7 |
| | FPA | 55.24 | | 98.98 | 0.7565 | 90.61 |
| | OTCA | 55.71 | | 99.82 | 0.071 | |
| Strong Partial Shading | TCA | 42.16 | 42.16 | 100 | 0.4972 | 86.7 |
| | FPA | 42.05 | | 99.74 | 0.7527 | 91.23 |
| | OTCA | 42.15 | | 99.98 | 0.066 | |

5. Two PV Strings Connected in Parallel (4S-2P)

The PV system configuration of two strings were connected in parallel to form a PV array. Each PV string possesses four series-connected PV modules. The 4S2P PV system configuration is depicted in Figure 12. The same irradiation levels described for the 4S PV system are applied for the 4S2P PV system.

5.1. Zero Partial Shading at 4S2P PV System (Test Case 1)

The P–V and I–V characteristic curves of the 4S2P PV system configuration for test case 1 are displayed in Figure 13. The ratings of the PV array at MPP, displayed in Figure 13, are 40 V, 6 A, and 240 W. The P–V characteristic curve describes the maximum power that could be extracted for the given conditions of the 4S2P PV system, which is 240 W.

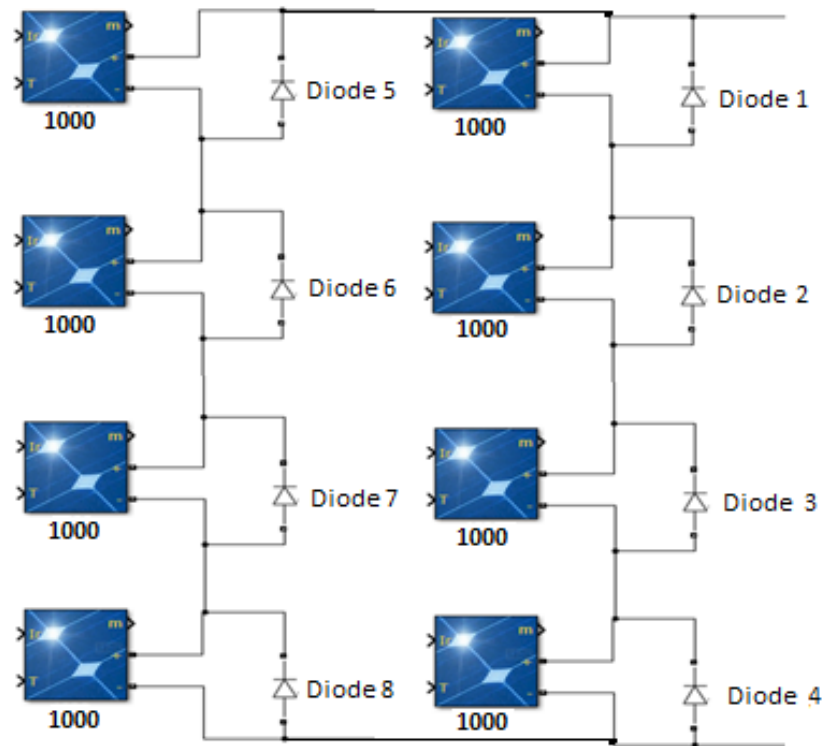


Figure 12. Test cases for 4S2P PV system configuration.

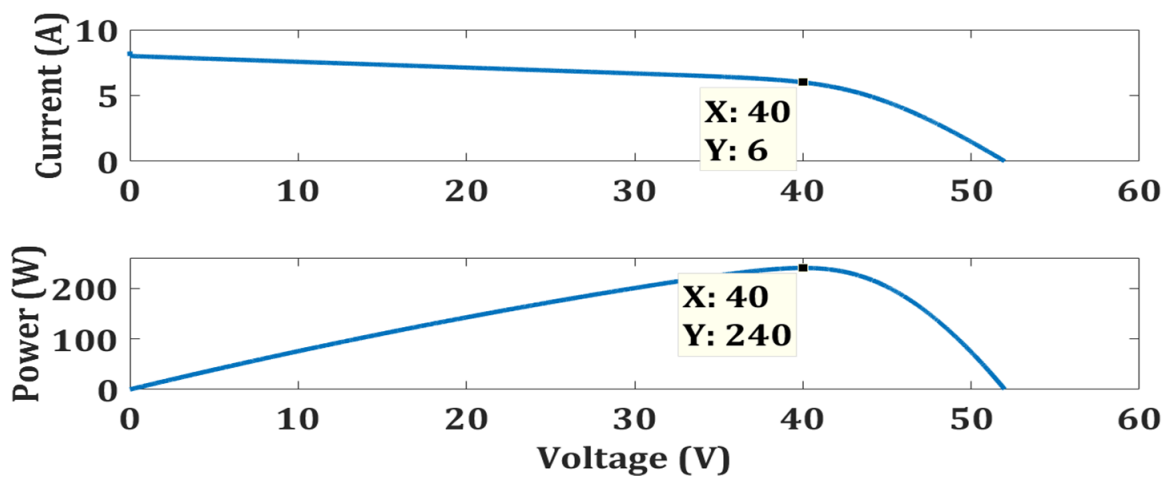


Figure 13. Characteristic curves of 4S2P PV system for test case 1.

5.2. Weak Partial Shading at 4S2P PV System (Test Case 2)

The P–V characteristic curve for test case 2 of a 4S2P PV system is depicted in Figure 14. Ratings of the GMPP, described in Figure 14, are 18.71 V, 5.966 A, and 111.6 W. The P–V characteristic curve describes the maximum power that could be extracted for the given conditions of the 4S2P PV system, which is 111.6 W.

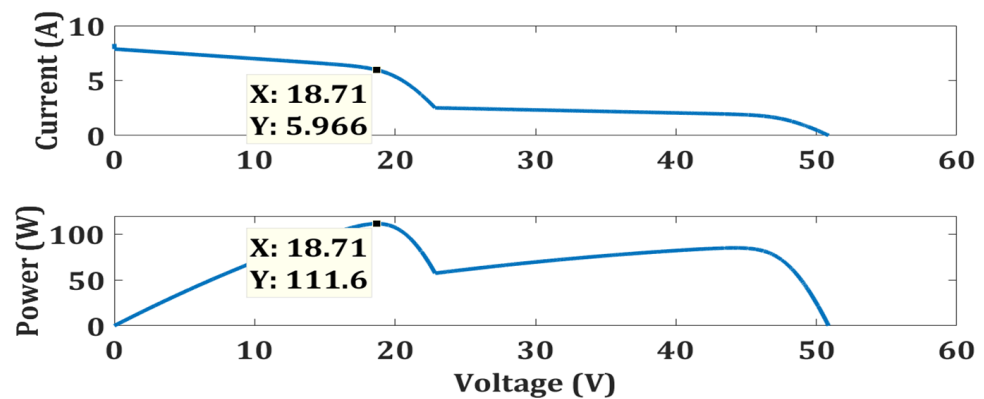


Figure 14. Characteristic curves of 4S2P PV system for test case 2.

5.3. Strong Partial Shading Condition at 4S2P PV System

The P–V characteristic curve for test case 3 of a 4S2P PV system is depicted in Figure 15. Ratings of the GMPP, described in Figure 15, are 43.85 V, 1.923 A, and 84.32 W. The P–V characteristic curve describes the maximum power that could be extracted for the given conditions of the 4S2P PV system, which is 84.32 W.

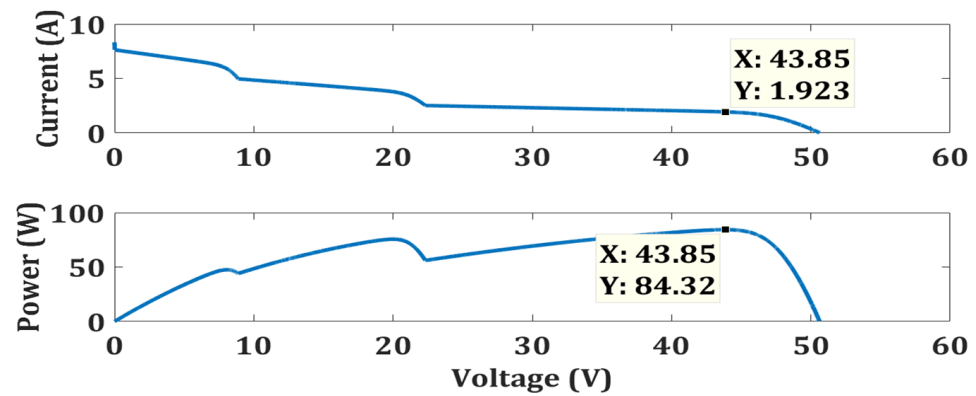


Figure 15. Characteristic curve of 4S2P PV system for test case 3.

The simulation result in Figure 16 has shown that the proposed OTCA algorithm extracted 239.9 W with 99.96% efficiency in 0.0705 s for test case 1, it converged at 110.4 W with an efficiency of 98.92% in 0.0798 s for test case 2, and it extracted 84.29 W with 100% efficiency in 0.0671 s for test case 3.

The simulation results have proven the performance of the OTCA algorithm in test case 1, test case 2, and test case 3 for a 4S2P PV system. The summary of the results is presented in Table 7.

Table 7. Performance comparison of OTCA for 4S2P PV system for all test cases.

| Partial Shading | Algorithms | Algorithms | Structural Complexity | Power (W) | Rated Power (W) | Efficiency (%) | Tracking Speed (s) |
|-----------------|------------|------------|-----------------------|-----------|-----------------|----------------|--------------------|
| Test Case 1 | OTCA | Ten Check | Simple | 239.9 | 240 | 99.96 | 0.0705 |
| Test Case 2 | OTCA | Ten Check | Simple | 110.4 | 111.6 | 98.92 | 0.0798 |
| Test Case 3 | OTCA | Ten Check | Simple | 84.29 | 84.32 | 99.96 | 0.0671 |

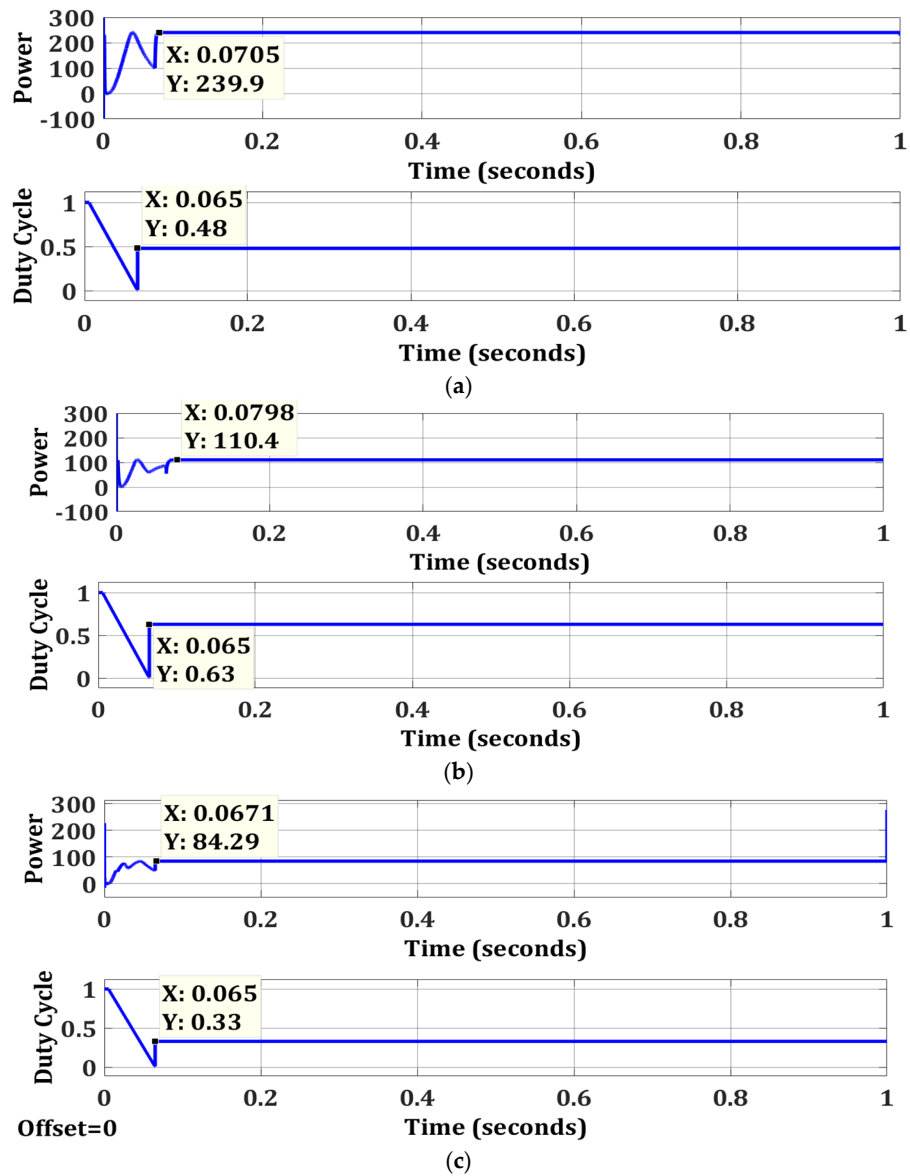


Figure 16. Simulation results for a 4S2P PV system: (a) ten check algorithm for test case 1; (b) ten check algorithm for test case 2; (c) ten check algorithm for test case 3.

5.4. Changing Weather Conditions for 4S2P PV System

The proposed OTCA algorithm detects the change in weather conditions and retains its performance under all weather conditions. This success story is present in Figure 17.

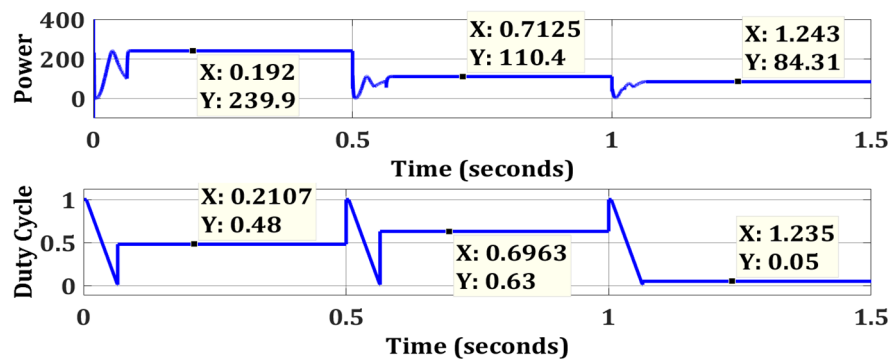


Figure 17. Changing weather conditions for 4S2P PV system configuration.

6. Three PV Modules Connected in Series (3S)

The PV system configuration of three modules is connected in series to form a PV string. The 3S PV system configuration for each test case is depicted in Figure 18. In test case 1, each PV module is receiving 1000 W/m². In test case 2, they are receiving 1000, 1000 and 500 W/m², separately. Whereas, in test case 3, they are receiving 1000, 750 and 500 W/m², separately.

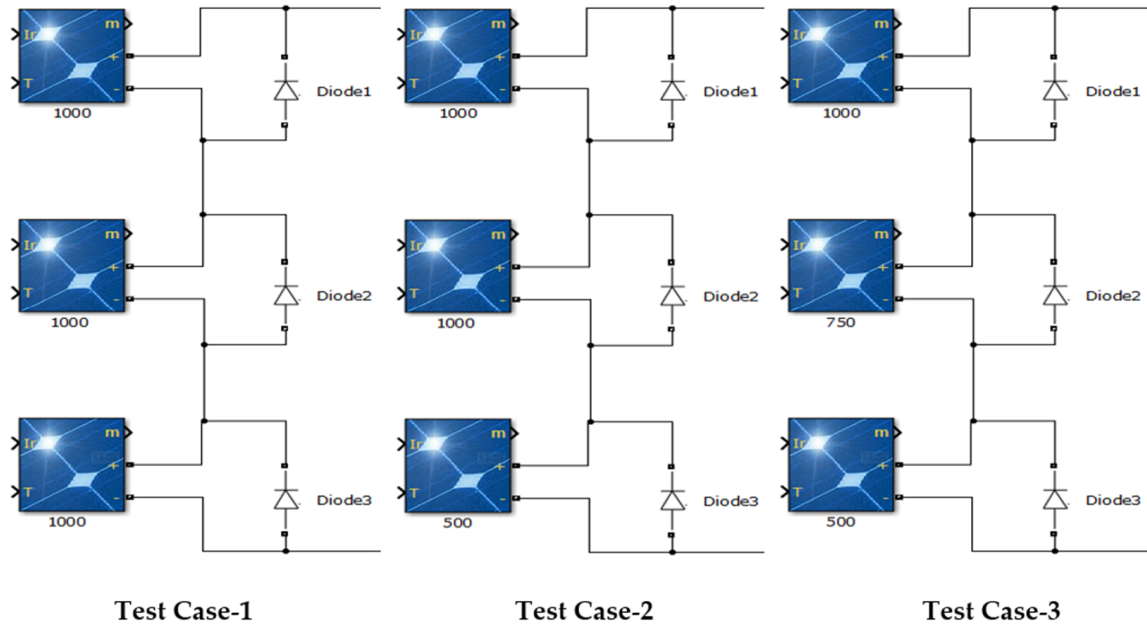


Figure 18. Test cases for 3S PV system.

6.1. Zero Shading at 3S PV system (Test Case 1)

The P–V and I–V characteristic curves of the 3S PV system for test case 1 are displayed in Figure 19. Ratings of the PV array at MPP, displayed in Figure 19, are 30 V, 3 A, and 90 W. The P–V characteristic curve describes the maximum power that could be extracted for the given conditions of a 3S PV system, which is 90 W.

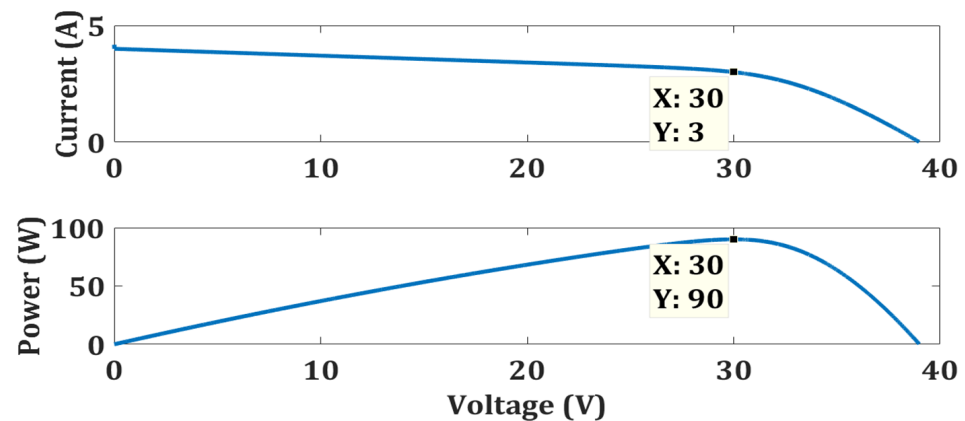


Figure 19. Characteristic curves of 3S PV system for test case 1.

6.2. Weak Partial Shading at 3S PV System (Test Case 2)

The P–V characteristic curve of the 3S PV system for test case 2 is depicted in Figure 20. Ratings of GMPP described in Figure 20 are 19.36 V, 2.991 A, and 57.9 W. The P–V characteristic curve describes the maximum power that could be extracted for the given conditions of the 3S PV system, which is 57.9 W.

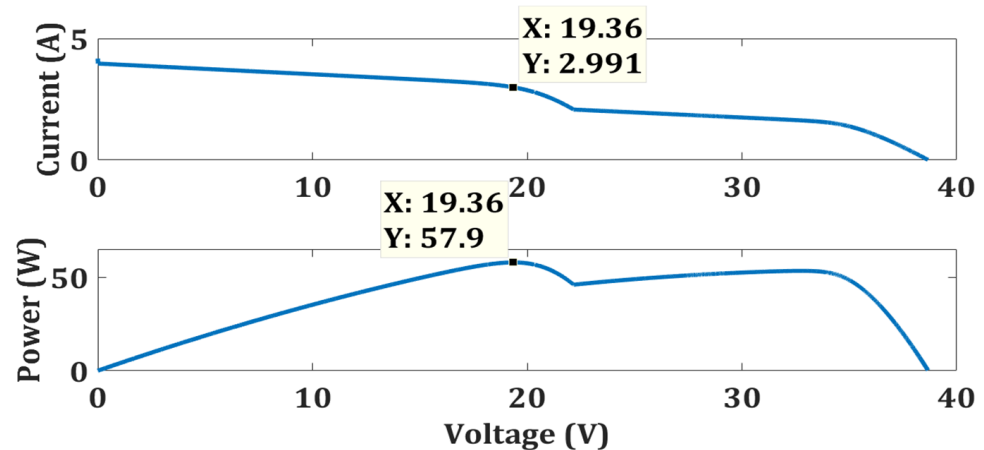


Figure 20. Characteristic curves of 3S PV system for test case 2.

6.3. Strong Partial Shading Condition at 3S PV System

The P–V characteristic curve of a 3S PV system for test case 3 is depicted in Figure 21. Ratings of the GMPP described in Figure 21 are 32.41 V, 1.63 A, and 52.83 W.

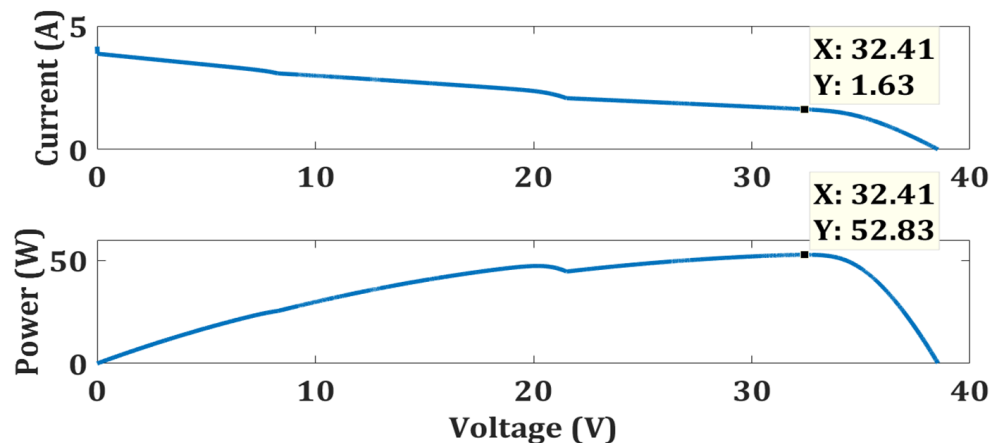


Figure 21. Characteristic curve of 3S PV system for test case 3.

The simulation results in Figure 22 show that the proposed OTCA algorithm extracted 89.98 W with 99.98% efficiency in 0.069 s for test case 1, it converged at 57.83 W with an efficiency of 99.88% in 0.0732 s for test case 2, and it has extracted 52.81 W with 99.96% efficiency in 0.0675 s for test case 3.

The simulation results have validated the performance of the proposed OTCA algorithm in test case 1, test case 2, and test case 3 for a 3S PV system. The summary of the results is presented in Table 8.

Table 8. Performance comparison of OTCA for 3S PV system for all test cases.

| Partial Shading | Algorithms | Structural Complexity | Oscillations | Power (W) | Rated Power (W) | Efficiency (%) | Tracking Speed (s) |
|-----------------|------------|-----------------------|--------------|-----------|-----------------|----------------|--------------------|
| Case 1 | OTCA | Simple | No | 89.98 | 90 | 99.98 | 0.069 |
| Case 2 | OTCA | Simple | No | 57.83 | 57.9 | 99.88 | 0.0732 |
| Case 3 | OTCA | Simple | No | 52.81 | 52.83 | 99.96 | 0.065 |

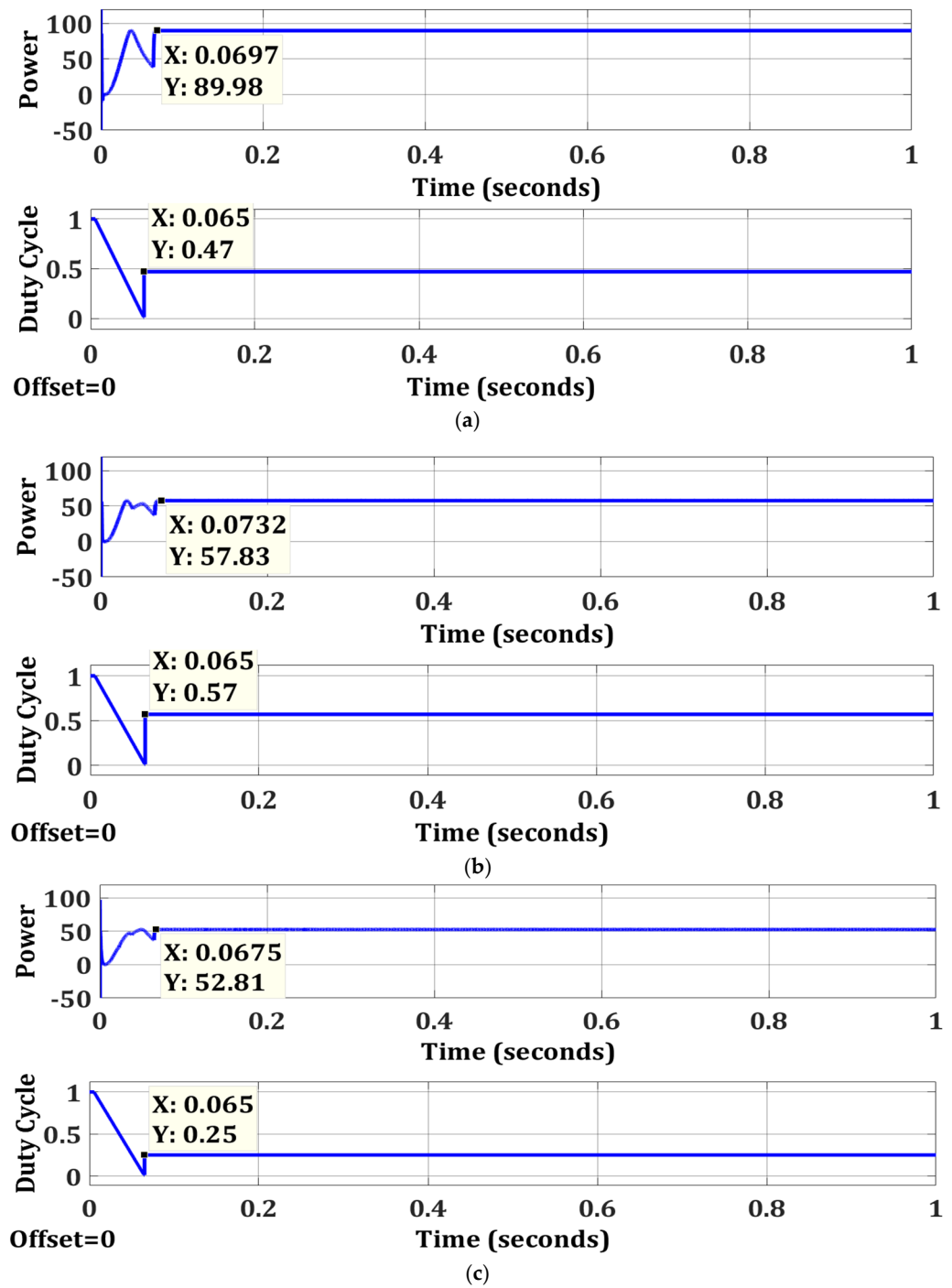


Figure 22. Simulation results for 3S PV system: (a) ten check algorithm for test case 1; (b) ten check algorithm for test case 2; (c) ten check algorithm for test case 3.

6.4. Changing Weather Conditions for 3S PV System

The proposed OTCA algorithm detects the change in weather conditions and retains its performance under all weather conditions. This success story is present in Figure 23.

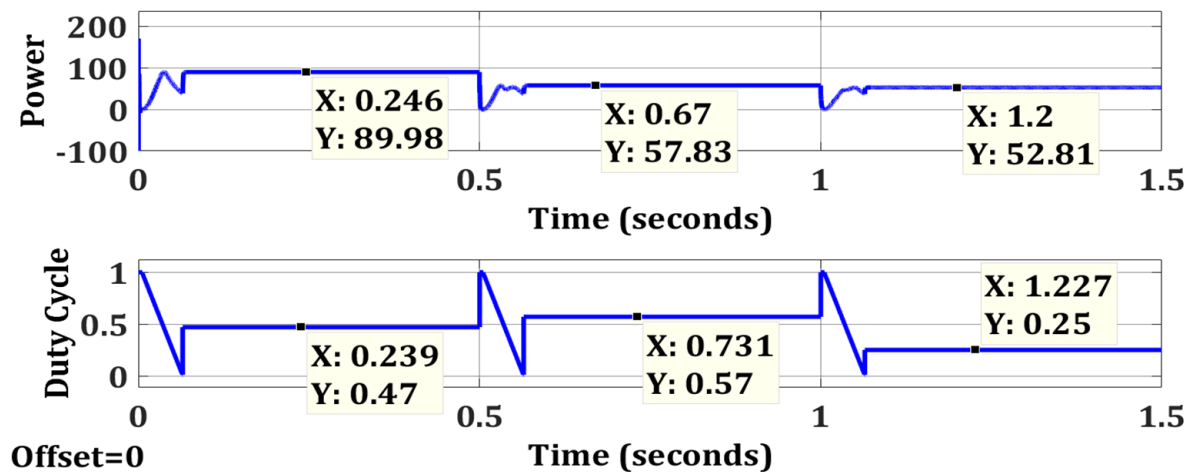


Figure 23. Changing weather condition for 3S PV system.

7. Two PV Strings Connected in Parallel (3S-2P)

The PV system configuration of two strings is connected in parallel to form a PV array. Each PV string possesses three series-connected PV modules. The 3S2P PV system configuration is depicted in Figure 24. The same irradiation levels described for the 3S PV system are applied for the 3S2P PV system.

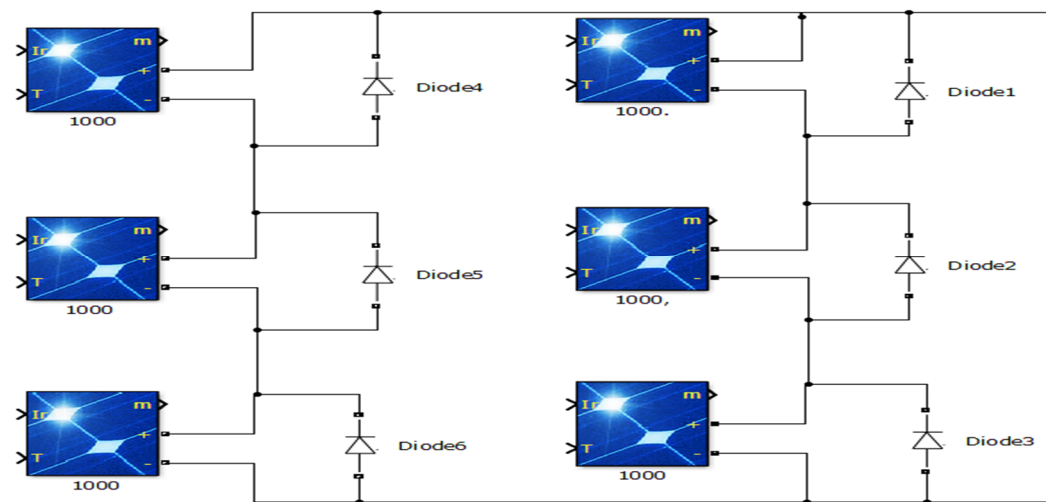


Figure 24. Test cases for 3S2P PV system configuration.

7.1. No Shading at the PV System (Test Case 1)

The P–V and I–V characteristic curves for test case 1 of a 3S2P PV system are displayed in Figure 25. The ratings of the PV array at MPP, displayed in Figure 25, are 30 V, 6 A, and 180 W. The P–V characteristic curve describes the maximum power that could be extracted for the given conditions of a 3S2P PV system, which is 180 W.

7.2. Weak Partial Shading at 3S2P PV System (Test Case 2)

The P–V characteristic curve for test case 2 of a 3S2P PV system is depicted in Figure 26. Ratings of GMPP, described in Figure 26, are 19.36 V, 5.982 A, and 115.8 W. The P–V characteristic curve describes the maximum power that could be extracted for the given conditions of the 3S2P PV system, which is 115.8 W.

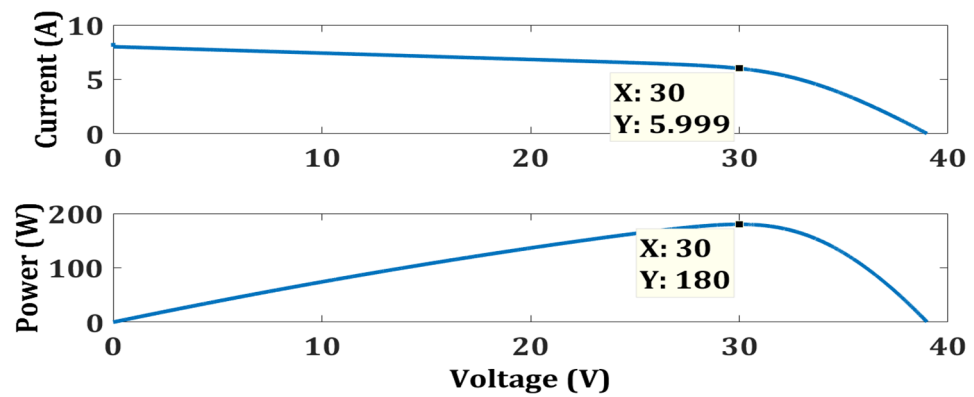


Figure 25. Characteristic curves of 3S2P PV system for test case 1.

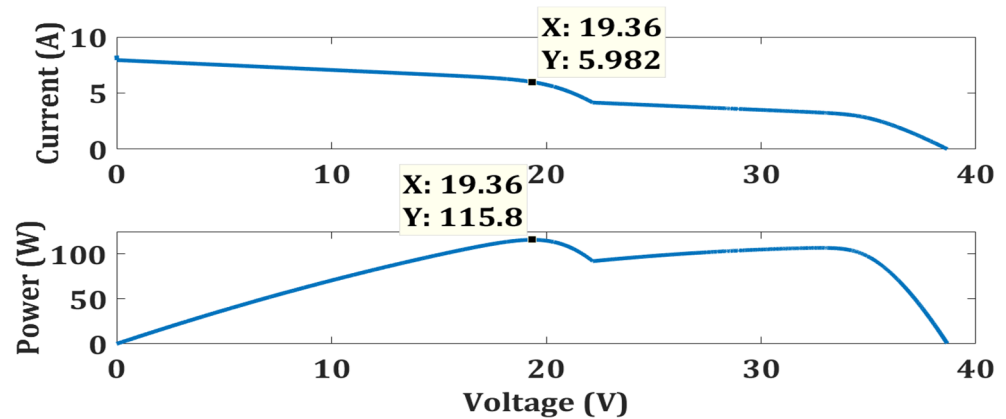


Figure 26. Characteristic curves of 3S2P PV system for test case 2.

7.3. Strong Partial Shading Condition (Test Case 3)

The P–V characteristic curve for test case 3 of a 3S2P PV system is depicted in Figure 27. Ratings of the GMPP, described in Figure 27, are 3.251 V, 2.983 A, and 105.6 W. The P–V characteristic curve describes the maximum power that could be extracted for the given conditions of the 3S2P PV system, which is 105.6 W.

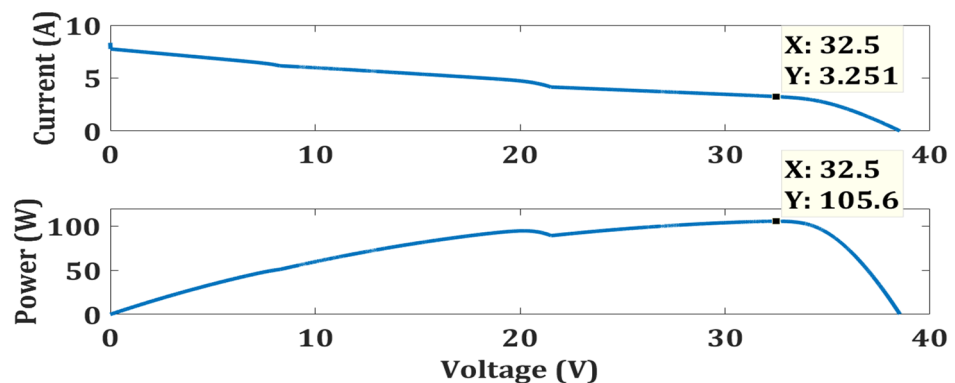


Figure 27. Characteristic curve of 3S2P PV system for test case 3.

The simulation results in Figure 28 show that the proposed OTCA algorithm extracted 179.4 W with 99.67% efficiency in 0.0721 s for test case 1, it converged at 114.7 W with an efficiency of 99.05% in 0.0753 s for test case 2, and extracted 105.6 W with 100% efficiency in 0.0688 s for test case 3.

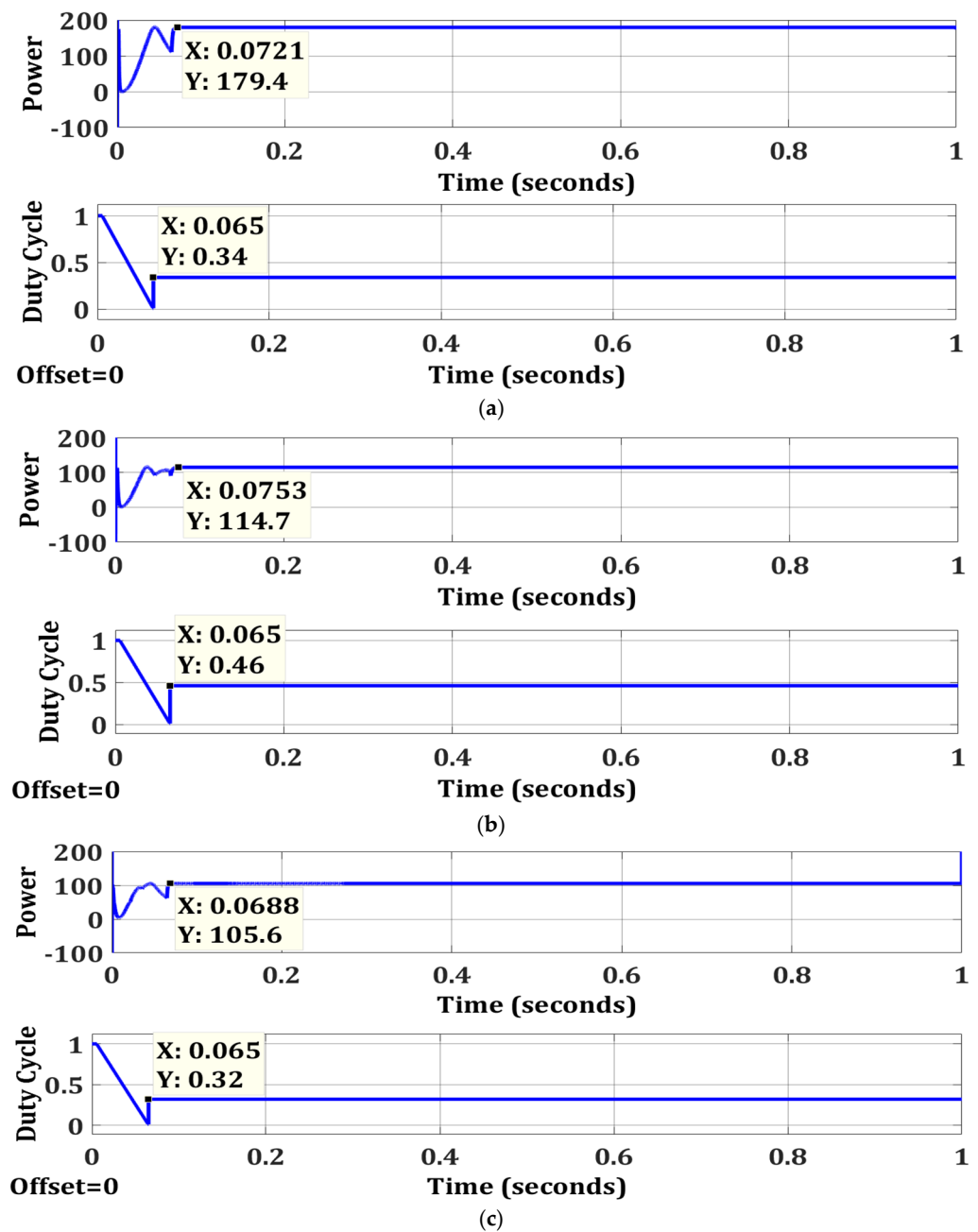


Figure 28. Simulation results for 3S2P PV system: (a) ten check algorithm for test case 1; (b) ten check algorithm for test case 2; (c) ten check algorithm for test case 3.

The simulation results have validated the performance of the proposed OTCA algorithm in test case 1, test case 2, and test case 3 for a 3S2P PV system. The summary of the results is presented in Table 9.

Table 9. Performance comparison of OTCA for 3S2P PV system for all test cases.

| Partial Shading | Algorithms | Structural Complexity | Oscillations | Power (W) | Rated Power (W) | Efficiency (%) | Tracking Speed (sec) |
|-----------------|------------|-----------------------|--------------|-----------|-----------------|----------------|----------------------|
| Case 1 | OTCA | Simple | No | 179.4 | 180 | 99.67 | 0.0721 |
| Case 2 | OTCA | Simple | No | 114.7 | 115.8 | 99.05 | 0.0753 |
| Case 3 | OTCA | Simple | No | 105.6 | 105.6 | 100 | 0.0688 |

7.4. Changing Weather Conditions for 3S2P PV System

The proposed OTCA algorithm detects the change in weather conditions and retains its performance under all weather conditions. This success story is presented in Figure 29.

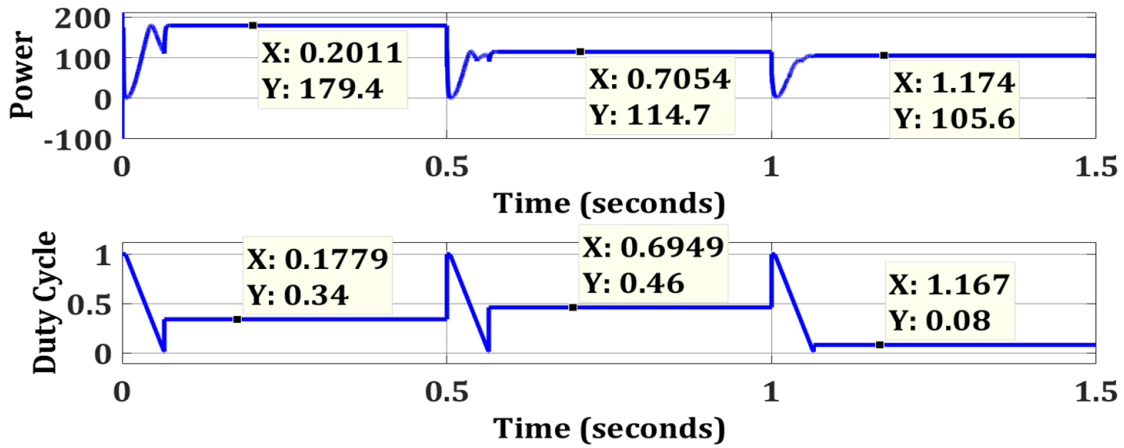


Figure 29. Changing weather conditions for 3S2P PV system configuration.

8. Two PV Modules Connected in Series (2S)

The PV system configuration of two modules is connected in series to form a PV string. The 2S PV system configuration for each test case is depicted in Figure 30. In test case 1, each PV module is receiving 1000 W/m². In test case 2, they are receiving 1000 W/m² and 500 W/m², separately, whereas in test case 3, they are receiving 800 W/m² and 500 W/m², separately.

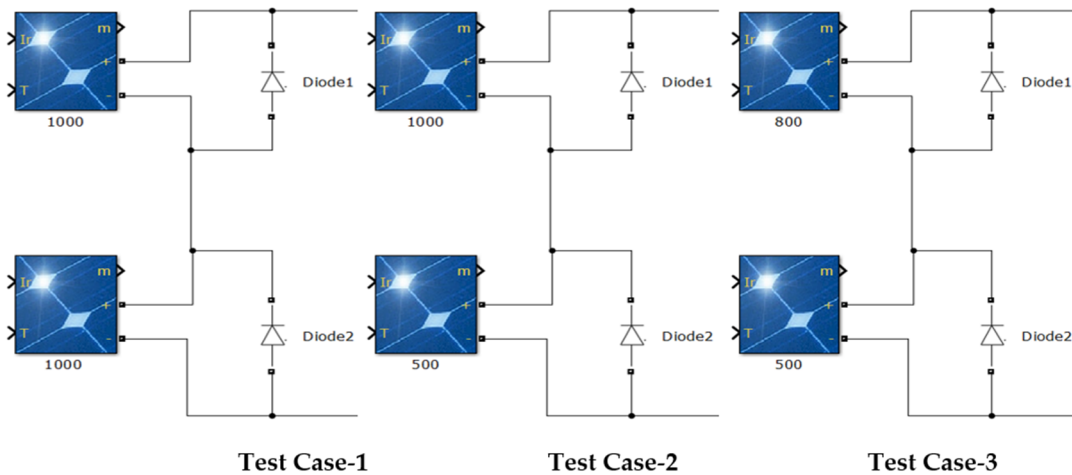


Figure 30. Test cases for 2S PV system.

8.1. Zero Shading at 2S PV System (Test Case 1)

In zero shading conditions, only one power peak emerges in the P–V curve. Thus, tracking MPP under this weather condition is an easy job. The P–V and I–V characteristic curves for test case 1 are displayed in Figure 31.

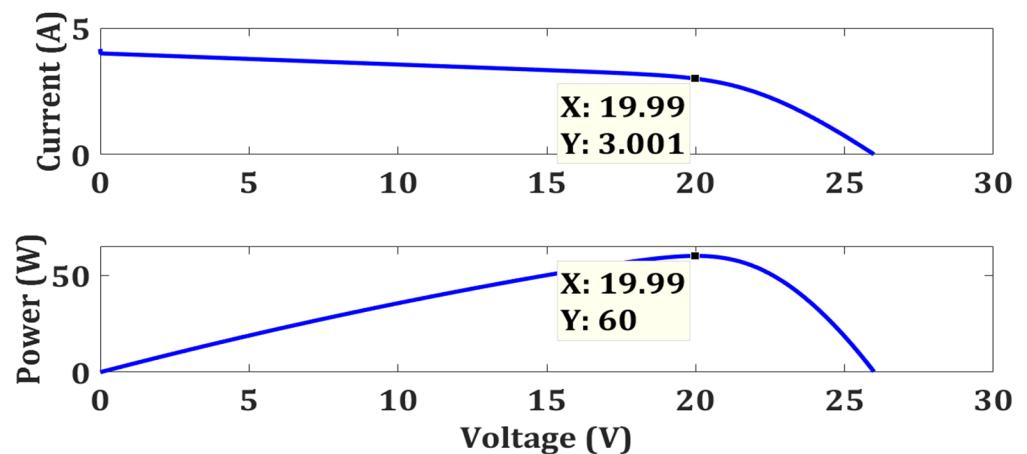


Figure 31. Characteristic curves of 2S PV system for test case 1.

The ratings of the PV array at MPP, displayed in Figure 31, are 19.99 V, 3.001 A, and 60 W. The P–V characteristic curve describes the maximum power that could be extracted for the given conditions of the 2S PV system, which is 60 W.

8.2. Weak Partial Shading at 2S PV System (Test Case 2)

Due to the formation of multiple power peaks, the structure of the P–V curve became complex, which complicated the identification of GMPP among LMPPs. The P–V characteristic curve of the 2S PV system for test case 2 is depicted in Figure 32. Ratings of the GMPP, described in Figure 32, are 21.61 V, 1.589 A, and 34.34 W. The P–V characteristic curve describes the maximum power that could be extracted for the given conditions of a 2S PV system, which is 34.34 W.

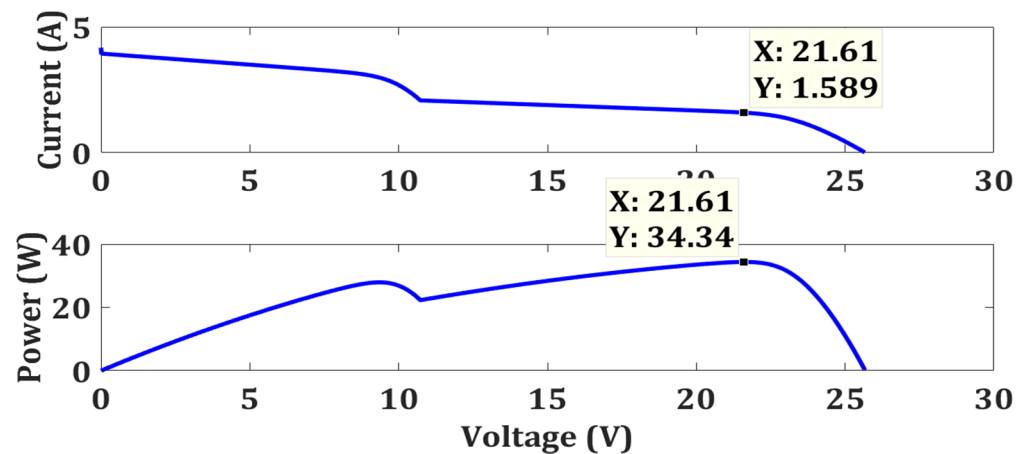


Figure 32. Characteristic curves of 2S PV system for test case 2.

8.3. Strong Partial Shading Condition at 2S PV System

Due to the formation of multiple power peaks, the structure of the P–V curve became complex, which complicated the identification of GMPP among LMPPs. The P–V characteristic curve of the 2S PV system for test case 3 is depicted in Figure 33. Ratings of the GMPP, described in Figure 33, are 21.4 V, 1.586 A, and 33.94 W. The P–V characteristic curve describes the maximum power that could be extracted for the given conditions of a 2S PV system, which is 33.94 W.

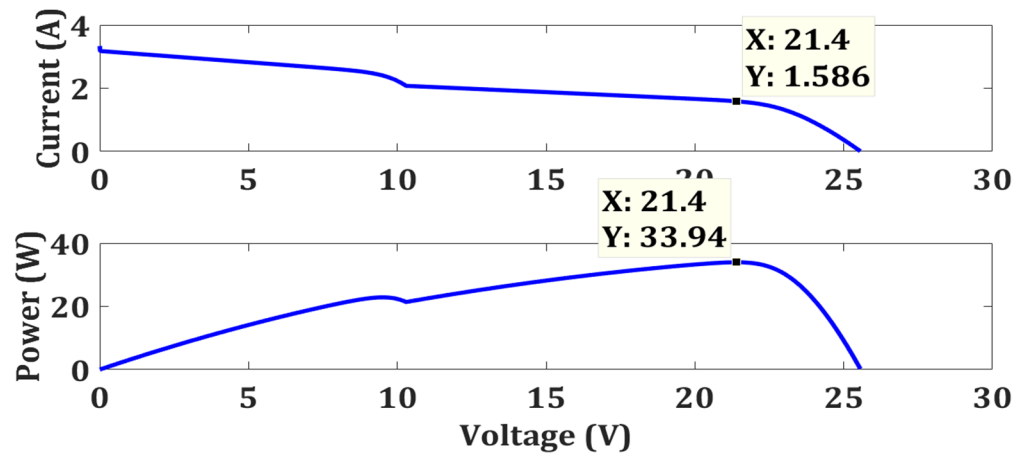


Figure 33. Characteristic curve of 2S PV system for test case 3.

The simulation results in Figure 34 show that the proposed OTCA algorithm extracted 59.99 W with 99.98% efficiency in 0.0711 s for test case 1, it converged at 34.34 W with 100% efficiency in 0.0674 s for test case 2, and it extracted 33.94 W with 100% efficiency in 0.067 s for test case 3.

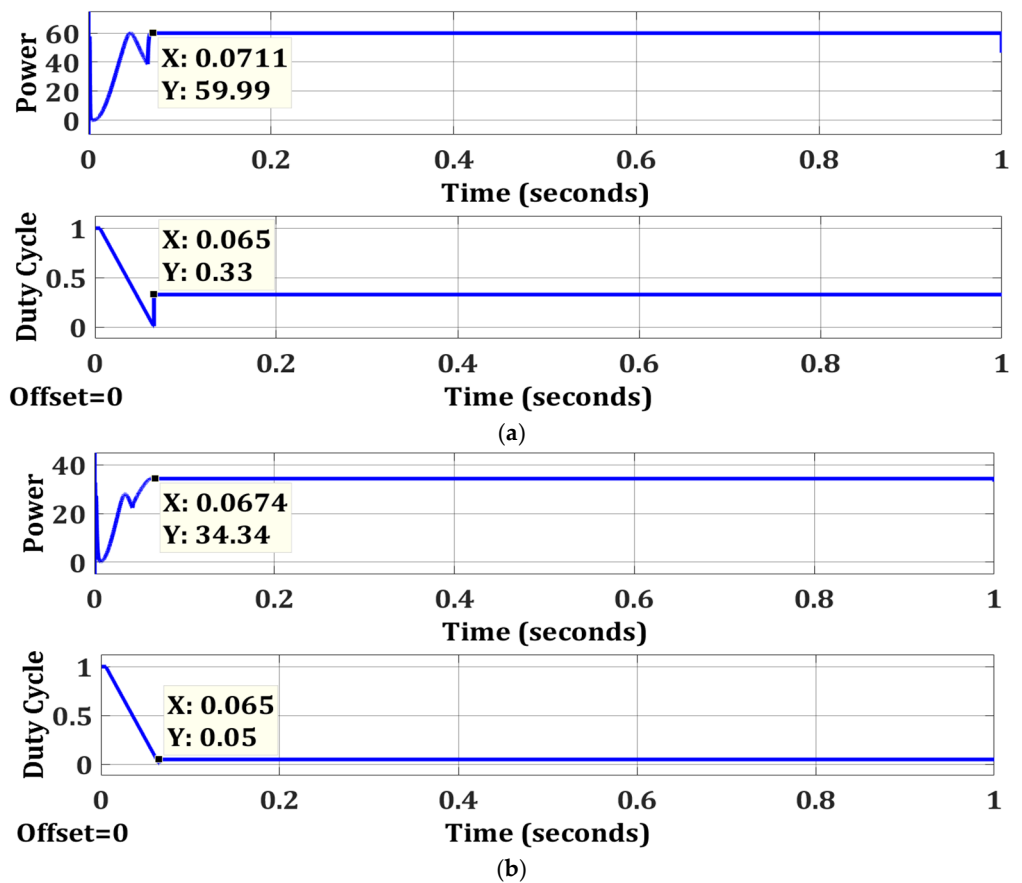


Figure 34. Cont.

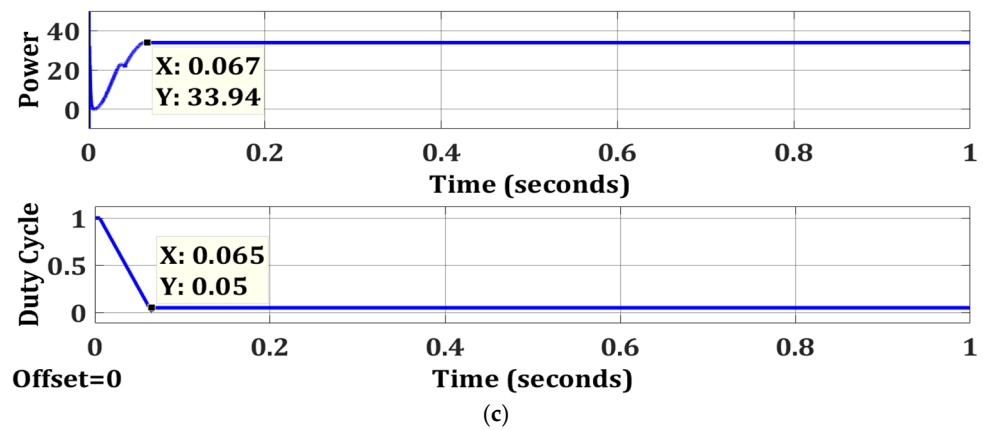


Figure 34. Simulation results for 2S PV system: (a) ten check algorithm for test case 1; (b) ten check algorithm for test case 2; (c) ten check algorithm for test case 3.

The simulation results have validated the performance of the proposed OTCA algorithm in test case 1, test case 2, and test case 3 for a 2S PV system. The summary of the results is presented in Table 10.

Table 10. Performance comparison of OTCA for 2S PV system for all test cases.

| Partial Shading | Algorithms | Structural Complexity | Oscillations | Power (W) | Rated Power (W) | Efficiency (%) | Tracking Speed (s) |
|-----------------|------------|-----------------------|--------------|-----------|-----------------|----------------|--------------------|
| Case 1 | OTCA | Simple | No | 59.99 | 60 | 99.98 | 0.0711 |
| Case 2 | OTCA | Simple | No | 34.34 | 34.34 | 100 | 0.0674 |
| Case 3 | OTCA | Simple | No | 33.94 | 33.94 | 100 | 0.067 |

8.4. Changing Weather Conditions for 2S PV System

The proposed OTCA algorithm detects the change in weather conditions and retains its performance under all weather conditions. This success story is present in Figure 35.

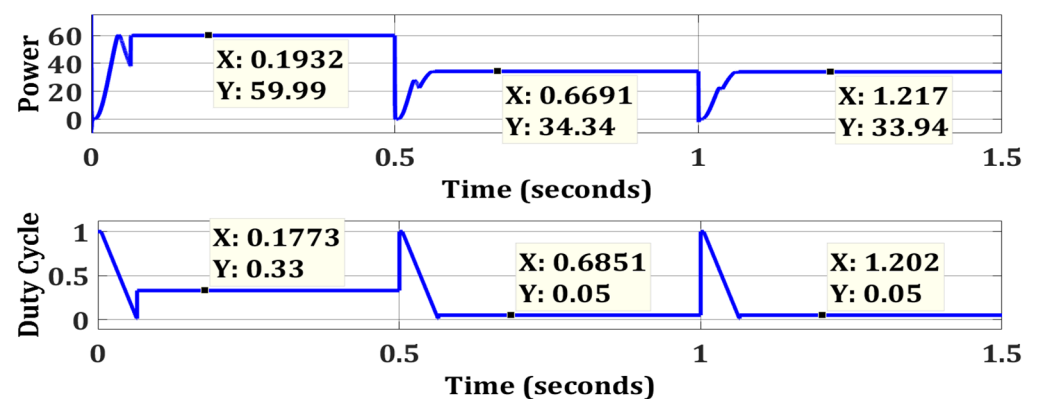


Figure 35. Changing weather conditions for 2S PV system.

9. Two PV Strings Connected in Parallel (2S-2P)

The PV system configuration of two strings is connected in parallel to form a PV array. Each PV string possesses two series-connected PV modules. The 2S2P PV system configuration is depicted in Figure 36. The same irradiation levels described for the 2S PV system are applied for the 2S2P PV system.

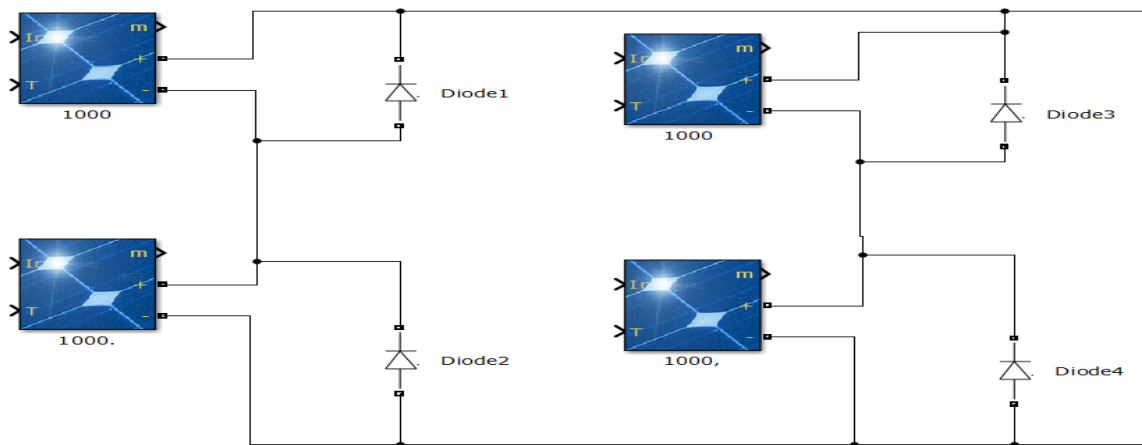


Figure 36. Test cases for 2S2P PV system configuration.

9.1. No Shading at the PV System (Test Case 1)

The P–V and I–V characteristic curves of the 2S2P PV system for test case 1 are displayed in Figure 37. The ratings of the PV array at MPP, displayed in Figure 37, are 19.99 V, 6.002 A, and 120 W. The P–V characteristic curve describes the maximum power that could be extracted for the given conditions of a 2S2P PV system, which is 120 W.

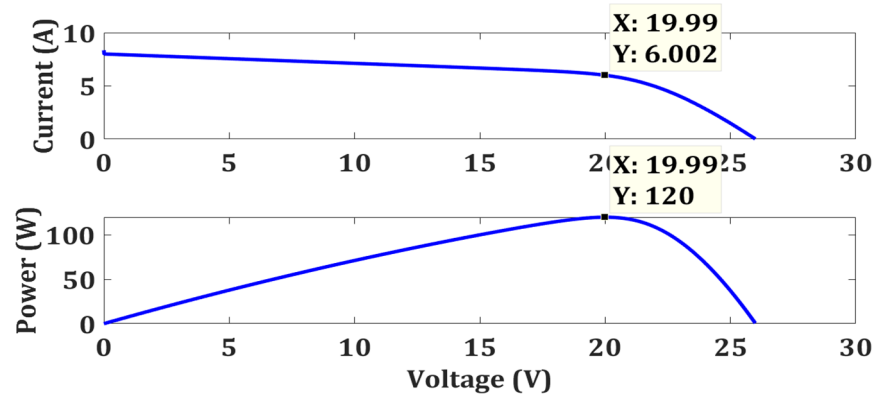


Figure 37. Characteristic curves of 2S2P PV system for test case 1.

9.2. Weak Partial Shading at 2S2P PV System (Test Case 2)

The P–V characteristic curve for test case 2 of a 2S2P PV system is depicted in Figure 38. Ratings of the GMPP, described in Figure 38, are 21.61 V, 3.179 A, and 68.67 W.

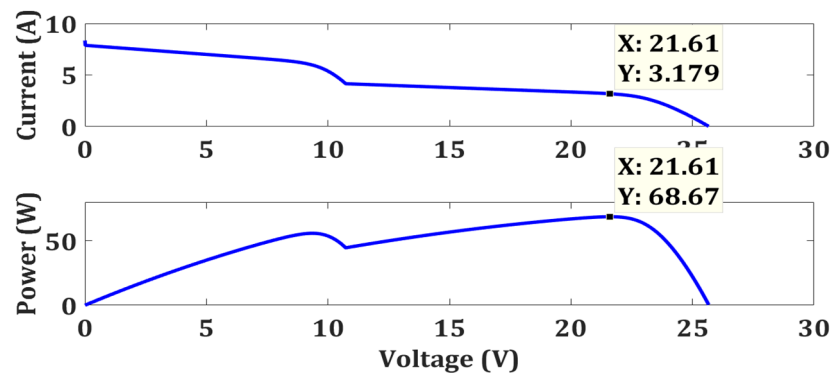


Figure 38. Characteristic curves of 2S2P PV system for test case 2.

9.3. Strong Partial Shading Condition (Test Case 3)

The P–V characteristic curve for test case 3 of a 2S2P PV system is depicted in Figure 39. Ratings of the GMPP, described in Figure 39, are 21.4 V, 3.172 A, and 67.88 W. The P–V characteristic curve describes the maximum power that could be extracted for the given conditions of the 2S2P PV system, which is 67.88 W.

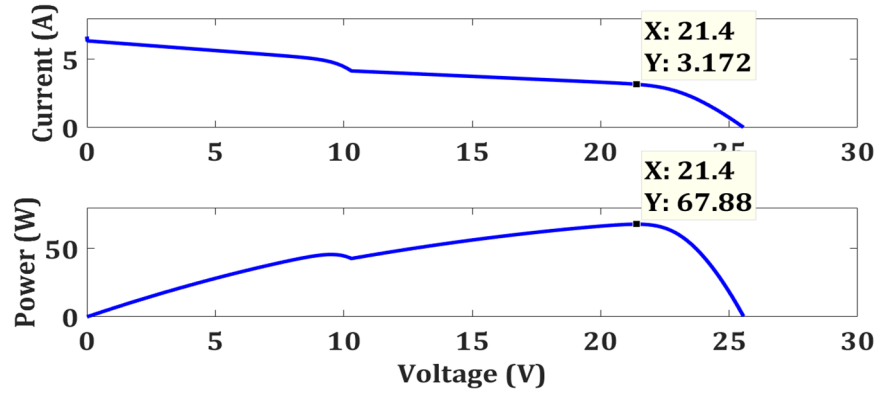


Figure 39. Characteristic curve of 2S2P PV system for test case 3.

The simulation results in Figure 40 show that the proposed OTCA algorithm extracted 118.3 W with 98.58% efficiency in 0.0786 s for test case 1, it converged at 68.63 W with an efficiency of 99.94% in 0.0722 s for test case 2, and it extracted 67.78 W with 99.85% efficiency in 0.0722 s for test case 3.

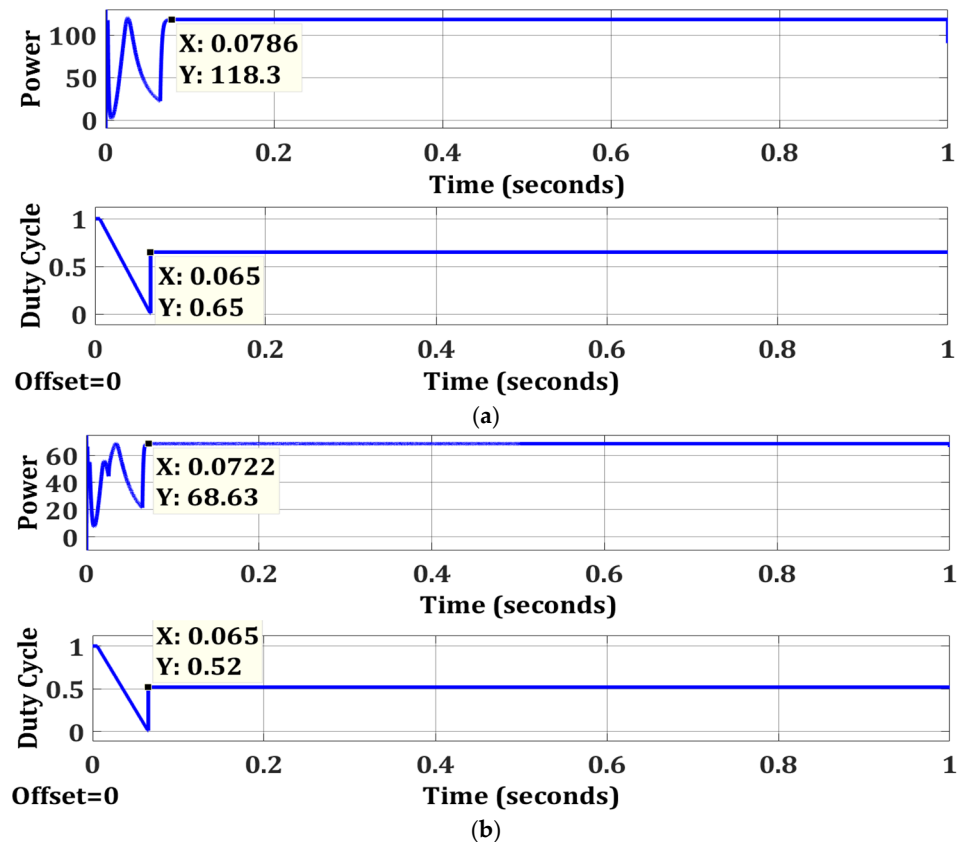


Figure 40. Cont.

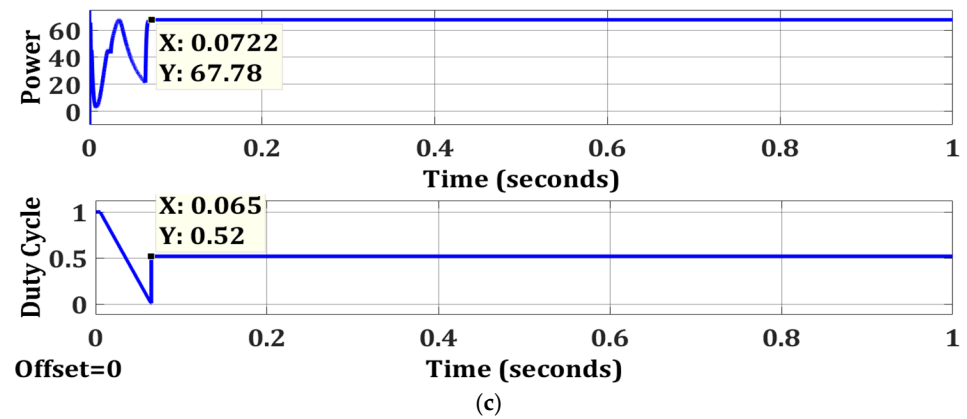


Figure 40. Simulation results for 2S2P PV system: (a) ten check algorithm for test case 1; (b) ten check algorithm for test case 2; (c) ten check algorithm for test case 3.

The simulation results have validated the performance of the proposed OTCA algorithm in test case 1, test case 2, and test case 3 for a 2S2P PV system. The summary of the results is presented in Table 11.

Table 11. Performance comparison of OTCA for 2S2P PV system for all test cases.

| Partial Shading | Algorithms | Structural Complexity | Oscillations | Power (W) | Rated Power (W) | Efficiency (%) | Tracking Speed (sec) |
|-----------------|------------|-----------------------|--------------|-----------|-----------------|----------------|----------------------|
| Case 1 | OTCA | Simple | No | 118.3 | 120 | 98.58 | 0.0786 |
| Case 2 | OTCA | Simple | No | 68.63 | 68.67 | 99.94 | 0.0722 |
| Case 3 | OTCA | Simple | No | 67.78 | 67.88 | 99.85 | 0.0722 |

9.4. Changing Weather Conditions for 2S2P PV System

The proposed OTCA algorithm detects the change in weather conditions and retains its performance under all weather conditions. This success story is present in Figure 41. The proposed algorithm maintained its performance efficiency and MPPT speed under dynamically changing weather conditions, which demonstrated its suitability for MPPT in solar PV systems operating under changeable weather conditions. Under broader assessment criteria, the performance was further verified using the standard benchmarks and was compared with leading conventional and soft-computing MPPT algorithms, as presented in Table 12.

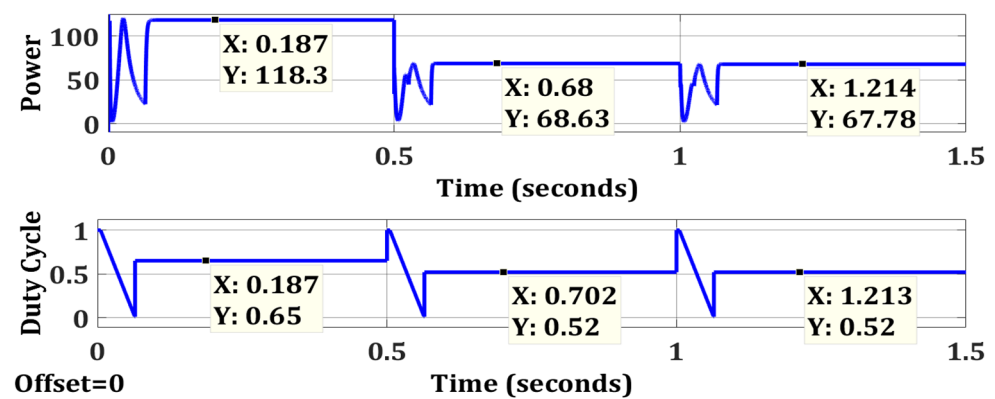


Figure 41. Changing weather conditions for 2S2P PV system configuration.

Table 12. Performance assessment of OTCA compared to leading MPPT algorithms.

| Sr. NO. | Algorithms | | | | | | |
|---------|-----------------------------|------------|-----------|-------------|---------------|------------|-----------|
| | Parameters | FPA [4] | TCA [37] | P&O [38,39] | Fuzzy [40] | PSO [41] | OTCA |
| 1 | Steady State Oscillations | Zero | Zero | High | Low | Zero | Zero |
| 2 | Tracking Speed | Fast | Faster | Low | Adequate | Adequate | FASTEST |
| 3 | Procedural Complications | Reasonable | Nil | Less | High | Reasonable | Nil |
| 4 | Memorizing Necessity | Few | Few | Few | Large | Few | FEW |
| 5 | Computational Complications | Average | No | Zero | High | Average | No |
| 6 | Implementation | Hard | Moderate | Easy | Hard | Hard | Easy |
| 7 | Performance in PSC | Good | Very Good | N/A | Good | Good | EXCELLENT |
| 8 | Module Dependent | No | No | Yes | Yes | No | No |
| 9 | Efficiency | Effective | High | Fail | Low under PSC | Effective | Exciting |
| 10 | Structure | Complex | Simple | Simple | Complex | Complex | Simple |

10. Conclusions

After evaluating the performance of conventional and soft-computing MPPT algorithms, it became clear that conventional algorithms are outperformed under partial shading conditions. However, the existing structural complexities, high cost, huge computational and memory requirements, extensive data training, and implementation complications all limit the practical efficiency, performance, and market presence of soft-computing MPPT algorithms. Most of these issues can be successfully resolved by employing the ten check algorithm (TCA). Based on the SWOT analysis conducted for TCA, it was observed that the main challenges faced by the algorithm revolve around settling time and tracking speed. After observing the inner relation of issues, it was concluded that reducing the settling could help in increasing the speed. Therefore, we have proposed a data arrangement technique and implemented it using the TCA algorithm to overcome the weaknesses associated with the TCA to avail of the opportunities that lie inside. The performance comparison of the proposed OTCA algorithm with the TCA and a well-established metaheuristic FPA algorithm was conducted under numerous shading patterns (zero shading/non-shading, weak partial shading, strong partial shading, and continuously changing weather conditions). The remarkable results were achieved with the proposed OTCA in terms of MPP tracking speed, efficiency, and settling time, as compared to TCA and FPA. An almost 86% and 90% increase in MPPT speed was recorded for OTCA vis à vis TCA and FPA, respectively. Additionally, the comparison between FPA, TCA, and the proposed OTCA algorithms was conducted for 10 different standard benchmarks, including structure, procedures, computations, oscillations, implementation, memory, efficiency, system dependency, tracking speed, and performance under static and variable shading conditions. The proposed OTCA clearly proved its superiority over both FPA and TCA in terms of all the standard benchmarks.

In the future, we plan to implement the proposed technique on a hardware based experimental setup using the dSPACE 1104 board. The results can also be tested using a dsPIC microcontroller or by field-programmable gate array (FPGA) implementation. Furthermore, we might investigate the possibility of operating a solar photovoltaic system at its maximum power point without MPP tracking. One hopes that there should be some mechanism capable of continuously operating the PV system at its MPP without putting it through the whole mess of MPP trackers and algorithms.

Author Contributions: Conceptualization, M.M.A.A., M.Y.J. and A.B.A.; methodology, M.M.A.A., M.Y.J. and A.B.A.; software, M.M.A.A.; validation, M.Y.J., A.B.A. and K.E.; formal analysis, M.Y.J., A.B.A. and K.E.; investigation, M.M.A.A., M.Y.J., A.B.A. and K.E.; resources, A.B.A. and K.E.; data curation, M.M.A.A., M.Y.J. and A.B.A.; writing—original draft preparation, M.M.A.A.; writing—review and editing, A.B.A. and K.E.; visualization, M.M.A.A., M.Y.J., A.B.A. and K.E.; supervision, M.Y.J., A.B.A. and K.E.; project administration, M.Y.J., A.B.A. and K.E.; funding acquisition, A.B.A. and K.E. All authors have read and agreed to the published version of the manuscript.

Funding: This research was funded by Polish National Agency for Academic Exchange under grant no. PPI/APM/2018/1/00047 entitled “Industry 4.0 in Production and Aeronautical Engineering” (International Academic Partnerships Program). The APC was funded by the Polish National Agency for Academic Exchange. The authors also want to offer their thanks for the substantive support provided by the KITT4SME (platform-enabled KITTs of artificial intelligence for an easy uptake by SMEs) project. The project was funded by the European Commission H2020 Program, under GA 952119.

Institutional Review Board Statement: Not applicable.

Informed Consent Statement: Not applicable.

Data Availability Statement: The data will be available on request.

Conflicts of Interest: The authors declare no conflict of interest.

References

- Ahmadi, M.H.; Ghazvini, M.; Sadeghzadeh, M.; Nazari, M.A.; Kumar, R.; Naeimi, A.; Ming, T. Solar power technology for electricity generation: A critical review. *Energy Sci. Eng.* **2018**, *6*, 340–361. [\[CrossRef\]](#)
- Rajput, P.; Malvoni, M.; Manoj Kumar, N.; Sastry, O.S.; Jayakumar, A. Operational performance and degradation influenced life cycle environmental–economic metrics of mc-Si, a-Si and HIT photovoltaic arrays in hot semi-arid climates. *Sustainability* **2020**, *12*, 1075. [\[CrossRef\]](#)
- Khatibi, A.; Astaraei, F.R.; Ahmadi, M.H. Generation and combination of the solar cells: A current model review. *Energy Sci. Eng.* **2019**, *7*, 305–322. [\[CrossRef\]](#)
- Awan, M.M.A.; Mahmood, T. Optimization of maximum power point tracking flower pollination algorithm for a standalone solar photovoltaic system. *Mehran Univ. Res. J. Eng. Technol.* **2020**, *39*, 267. [\[CrossRef\]](#)
- Başoğlu, M.E. A Fast GMPPT Algorithm Based on PV Characteristic for Partial Shading Conditions. *Electronics* **2019**, *8*, 1142. [\[CrossRef\]](#)
- Awan, M.M.A.; Awan, F.G. Improvement of maximum power point tracking perturb and observe algorithm for a standalone solar photovoltaic system. *Mehran Univ. Res. J. Eng. Technol.* **2017**, *36*, 501–510. [\[CrossRef\]](#)
- Feroz Mirza, A.; Mansoor, M.; Ling, Q.; Khan, M.I.; Aldossary, O.M. Advanced variable step size incremental conductance MPPT for a standalone PV system utilizing a GA-tuned PID controller. *Energies* **2020**, *13*, 4153. [\[CrossRef\]](#)
- Basha, C.H.; Rani, C. Different conventional and soft computing MPPT techniques for solar PV systems with high step-up boost converters: A comprehensive analysis. *Energies* **2020**, *13*, 371. [\[CrossRef\]](#)
- Debnath, A.; Olowu, T.O.; Parvez, I.; Dastgir, M.G.; Sarwat, A. A novel module independent straight line-based fast maximum power point tracking algorithm for photovoltaic systems. *Energies* **2020**, *13*, 3233. [\[CrossRef\]](#)
- Salam, Z.; Ahmed, J.; Merugu, B.S. The application of soft computing methods for MPPT of PV system: A technological and status review. *Appl. Energy* **2013**, *107*, 135–148. [\[CrossRef\]](#)
- Abdelsalam, A.K.; Massoud, A.M.; Ahmed, S.; Enjeti, P.N. High-Performance Adaptive Perturb and Observe MPPT Technique for Photovoltaic-Based Microgrids. *IEEE Trans. Power Electron.* **2011**, *26*, 1010–1021. [\[CrossRef\]](#)
- Ahmed, J.; Salam, Z. An improved perturb and observe (P&O) maximum power point tracking (MPPT) algorithm for higher efficiency. *Appl. Energy* **2015**, *150*, 97–108.
- Ishaque, K.; Salam, Z. A review of maximum power point tracking techniques of PV system for uniform insolation and partial shading condition. *Renew. Sustain. Energy Rev.* **2013**, *19*, 475–488. [\[CrossRef\]](#)
- Bastidas-Rodriguez, J.D.; Spagnuolo, G.; Franco, E.; Ramos-Paja, C.A.; Petrone, G. Maximum power point tracking architectures for photovoltaic systems in mismatching conditions: A review. *IET Power Electron.* **2014**, *7*, 1396–1413. [\[CrossRef\]](#)
- Xiao, W.; Dunford, W.G. A modified adaptive hill climbing MPPT method for photovoltaic power systems. In Proceedings of the 2004 IEEE 35th Annual Power Electronics Specialists Conference (IEEE Cat. No.04CH37551), Aachen, Germany, 20–25 June 2004; Volume 3, pp. 1957–1963.
- Zhou, Y.; Liu, F.; Yin, J.; Duan, S. Study on realizing MPPT by improved incremental conductance method with variable step-size. In Proceedings of the 2008 3rd IEEE Conference on Industrial Electronics and Applications, Singapore, 3–5 June 2008; pp. 547–550.
- Necaibia, S.; Kelaiaia, M.S.; Labar, H.; Necaibia, A. Implementation of an improved incremental conductance MPPT control based boost converter in photovoltaic applications. *Int. J. Emerg. Electr. Power Syst.* **2017**, *18*. [\[CrossRef\]](#)

18. Sher, H.A.; Murtaza, A.F.; Noman, A.; Addoweesh, K.E.; Al-Haddad, K.; Chiaberge, M. A new sensorless hybrid MPPT algorithm based on fractional short-circuit current measurement and P&O MPPT. *IEEE Trans. Sustain. Energy* **2015**, *6*, 1426–1434.
19. Baimel, D.; Tapuchi, S.; Levron, Y.; Belikov, J. Improved Fractional Open Circuit Voltage MPPT Methods for PV Systems. *Electronics* **2019**, *8*, 321. [\[CrossRef\]](#)
20. Wang, Y.; Yang, Y.; Fang, G.; Zhang, B.; Wen, H.; Tang, H.; Fu, L.; Chen, X. An Advanced Maximum Power Point Tracking Method for Photovoltaic Systems by Using Variable Universe Fuzzy Logic Control Considering Temperature Variability. *Electronics* **2018**, *7*, 355. [\[CrossRef\]](#)
21. Ilyas, A.; Ayyub, M.; Khan, M.R. Modelling and simulation of MPPT techniques for solar photovoltaic system using genetic algorithm optimised fuzzy logic controller. *Int. J. Energy Technol. Policy* **2020**, *16*, 174–195. [\[CrossRef\]](#)
22. Basha, C.H.; Bansal, V.; Rani, C.; Brisilla, R.; Odofin, S. Development of Cuckoo Search MPPT Algorithm for Partially Shaded Solar PV SEPIC Converter. In *Soft Computing for Problem Solving*; Springer: Berlin/Heidelberg, Germany, 2020; pp. 727–736.
23. Kinattungal, S.; Simon, S.P.; Nayak, P.S.R. MPPT in PV systems using ant colony optimisation with dwindling population. *IET Renew. Power Gener.* **2020**, *14*, 1105–1112.
24. Tiwari, R.; Krishnamurthy, K.; Neelakandan, R.B.; Padmanaban, S.; Wheeler, P.W. Neural Network Based Maximum Power Point Tracking Control with Quadratic Boost Converter for PMSG—Wind Energy Conversion System. *Electronics* **2018**, *7*, 20. [\[CrossRef\]](#)
25. Algarín, C.R.; Hernández, D.S.; Leal, D.R. A Low-Cost Maximum Power Point Tracking System Based on Neural Network Inverse Model Controller. *Electronics* **2018**, *7*, 4. [\[CrossRef\]](#)
26. Zhang, P.; Sui, H. Maximum Power Point Tracking Technology of Photovoltaic Array under Partial Shading Based On Adaptive Improved Differential Evolution Algorithm. *Energies* **2020**, *13*, 1254. [\[CrossRef\]](#)
27. da Luz, C.M.A.; Vicente, E.M.; Tofoli, F.L. Experimental evaluation of global maximum power point techniques under partial shading conditions. *Sol. Energy* **2020**, *196*, 49–73. [\[CrossRef\]](#)
28. Wan, Y.; Mao, M.; Zhou, L.; Zhang, Q.; Xi, X.; Zheng, C. A Novel Nature-Inspired Maximum Power Point Tracking (MPPT) Controller Based on SSA-GWO Algorithm for Partially Shaded Photovoltaic Systems. *Electronics* **2019**, *8*, 680. [\[CrossRef\]](#)
29. Pilakkat, D.; Kanthalakshmi, S. Single phase PV system operating under Partially Shaded Conditions with ABC-PO as MPPT algorithm for grid connected applications. *Energy Rep.* **2020**, *6*, 1910–1921. [\[CrossRef\]](#)
30. Rajesh, R.; Mabel, M.C. Design and real time implementation of a novel rule compressed fuzzy logic method for the determination operating point in a photo voltaic system. *Energy* **2016**, *116*, 140–153. [\[CrossRef\]](#)
31. Khanaki, R.; Radzi, M.A.M.; Marhaban, M.H. Comparison of ANN and P&O MPPT methods for PV applications under changing solar irradiation. In Proceedings of the 2013 IEEE Conference on Clean Energy and Technology (CEAT), Langkawi, Malaysia, 18–20 November 2013; pp. 287–292.
32. Paul, S.; Thomas, J. Comparison of MPPT using GA optimized ANN employing PI controller for solar PV system with MPPT using incremental conductance. In Proceedings of the 2014 International Conference on Power Signals Control and Computations (EPSCICON), Thrissur, India, 6–11 January 2014; pp. 1–5.
33. Chen, X.; Li, Y. A modified PSO structure resulting in high exploration ability with convergence guaranteed. *IEEE Trans. Syst. Man Cybern. Part B (Cybern.)* **2007**, *37*, 1271–1289. [\[CrossRef\]](#)
34. Yousri, D.; Babu, T.S.; Allam, D.; Ramachandaramurthy, V.K.; Etiba, M.B. A Novel Chaotic Flower Pollination Algorithm for Global Maximum Power Point Tracking for Photovoltaic System under Partial Shading Conditions. *IEEE Access* **2019**, *7*, 121432–121445. [\[CrossRef\]](#)
35. Javed, M.Y.; Mirza, A.F.; Hasan, A.; Rizvi, S.T.H.; Ling, Q.; Gulzar, M.M.; Safder, M.U.; Mansoor, M. A Comprehensive Review on a PV Based System to Harvest Maximum Power. *Electronics* **2019**, *8*, 1480. [\[CrossRef\]](#)
36. Al-Majidi, S.D.; Abbod, M.F.; Al-Raweshidy, H.S. Design of an Efficient Maximum Power Point Tracker Based on ANFIS Using an Experimental Photovoltaic System Data. *Electronics* **2019**, *8*, 858. [\[CrossRef\]](#)
37. Awan, M.M.A.; Mahmood, T. A Novel Ten Check Maximum Power Point Tracking Algorithm for a Standalone Solar Photovoltaic System. *Electronics* **2018**, *7*, 327. [\[CrossRef\]](#)
38. Mousa, H.H.; Youssef, A.-R.; Mohamed, E.E. Variable step size P&O MPPT algorithm for optimal power extraction of multi-phase PMSG based wind generation system. *Int. J. Electr. Power Energy Syst.* **2019**, *108*, 218–231.
39. Balaji, V.; Fathima, A.P. Enhancing the Maximum Power Extraction in Partially Shaded PV Arrays using Hybrid Salp Swarm Perturb and Observe Algorithm. *Int. J. Renew. Energy Res. (IJRER)* **2020**, *10*, 898–911.
40. Zhang, S.; Wang, T.; Li, C.; Zhang, J.; Wang, Y. Maximum power point tracking control of solar power generation systems based on type-2 fuzzy logic. In Proceedings of the 2016 12th World Congress on Intelligent Control and Automation (WCICA), Guilin, China, 12–15 June 2016; pp. 770–774.
41. Miyatake, M.; Veerachary, M.; Toriumi, F.; Fujii, N.; Ko, H. Maximum power point tracking of multiple photovoltaic arrays: A PSO approach. *IEEE Trans. Aerosp. Electron. Syst.* **2011**, *47*, 367–380. [\[CrossRef\]](#)